# Discotic liquid crystals of transition metal complexes 49†: Establishment of helical structure of fullerene moieties in columnar mesophase of phthalocyanine-fullerene dyads

**Lisa Tauchi[a], Takahiro Nakagaki[a], Masahiro Shimizu[a], Eiji Itoh[b], Mikio Yasutake[c] and Kazuchika Ohta[a]***

[a]*Smart Material Science and Technology, Interdisciplinary Graduate School of Science and Technology, Shinshu University, 1-15-1 Tokida, Ueda, 386-8567, Japan;* [b]*Department of Electrical and Electronic Engineering, Shinshu University, 4-17-1 Wakasato, Nagano 380-8553, Japan;* [c]*Comprehensive Analysis Center for Science, Saitama University,255 Shimo-okubo, Sakura-ku, Saitama 338-8570, Japan.*

*Received date (to be automatically inserted after your manuscript is submitted)*
*Accepted date (to be automatically inserted after your manuscript is accepted)*

**ABSTRACT:** A homologous series of the phthalocyanine-fullerene dyads, **$C_n$-PcM(OFbaC$_{60}$)** (n=6,8,10,12; M=Cu, Ni, Co: **3a**~**f**), have been synthesized to obtain homeotropic alignment at rt and investigate the effects of spacer chain length (n=6,8,10,12) and central metal (M=Cu, Ni, Co) on the mesomorphism. Interestingly, the shorter-spacer-substituted (n=6, 8; M=Cu) dyads **3a**,**b** showed a hexagonal columnar mesophase ($Col_h$), whereas the longer-spacer-substituted (n=10, 12; M=Cu, Ni, Co) dyads **3c**~**f** showed a tetragonal columnar mesophase ($Col_{tet}$). Moreover, each of the homologues **3a**~**e** shows perfect homeotropic alignment in both the $Col_h$ and $Col_{tet}$ mesophases at rt. More interestingly, these columnar mesophases gave a very unique XRD reflection peak denoted as Peak H in a very small angle region of $0.8 < 2\theta < 2.0$ degree. We have established at the first time from our developed two new XRD sample preparation techniques that the Peak H is due to the helical structure of fullerenes around columns formed by one-dimensionally stacked Pc cores. 1D nano array structure of donor and acceptor between two electrodes is recently proposed to obtain higher photoelectric conversion efficiency for organic thin film solar cells. This 1D nano array structure is almost compatible with the present homeotropically aligned Pc-$C_{60}$ dyads **3a**~**f** between two glass plates. Hence, these novel Pc-$C_{60}$ dyads **3a**~**f** may be very suitable to organic thin film solar cells.

**KEYWORDS:** Discotic liquid crystal, phthalocyanine, fullerene, phthalocyanine-fullerene dyad, homeotropic alignment, organic thin film solar cell

*Correspondence to: Kazuchika Ohta, e-mail: ko52517@ shinshu-u.ac.jp

†Part 48, Masahiro Shimizu, Lisa Tauchi, Takahiro Nakagaki, Aya Ishikawa, Eiji Itoh and Kazuchika Ohta *J. Porphyrins Phthalocyanines*, 2013, in press.

## 1. INTRODUCTION

Liquid crystalline donor-acceptor (D-A) complexes may display superb performance in organic thin film solar cells [1-25]. They can greatly reduce their costs to manufacture the solar cells. Especially, columnar mesophases in homeotropic alignment are so favourable to obtain higher photoelectric conversion efficiency which can be attributable to larger π-π stacking of the π-conjugated macrocycles [19].

In 2001, we succeeded in synthesis of phthalocyanine derivatives showing perfect homeotropic alignment in large area at high temperatures [26]. Furthermore, in 2007 we reported the first liquid crystalline phthalocyanine-fullerene dyad, **PcCu(OMalC$_{60}$) (OCH$_3$)** (**1** in Fig. 1), exhibiting perfect homeotropic alignment in the hexagonal columnar phase (Col$_h$) at high temperatures [14]. For the synthesis of this phthalocyanine-fullerene dyad **1**, Bingel reaction [27] was adopted to connect phthalocyanine and fullerene. However, it gave polyads connected with two or three phthalocyanines per one fullerene, as the by-products at the same time. Accordingly, the yield of the target 1:1 phthalocyanine-fullerene dyad **1** was very low (20%). Therefore, we changed the synthetic method from Bingel reaction to Prato reaction [28]. By using Prato reaction, the 1:1 phthalocyanine-fullerene dyads, **PcM(OFbaC$_{60}$)(OCH$_3$)** (**2** in Fig. 1), could be synthesized in very high yield (81~96%) with negligible amount of undesirable 2:1 phthalocyanine-fullerene by-product [25]. Thus, Prato reaction was more favourable to obtain phthalocyanine-fullerene dyads than Bingel reaction. The Prato 1:1 phthalocyanine-fullerene dyads **2** also showed perfect homeotropic alignment in the tetragonal columnar phase (Col$_{tet}$) at high temperatures [25]. Recently, we successfully synthesized novel phthalocyanine-fullerene dyads, **C$_{12}$-PcCu(OFbaC$_{60}$)** (**3f** in Fig. 1), also by using Prato reaction and another commercially available starting material [29]. Very interestingly, the novel dyad **3f** shows perfect homeotropic alignment in the tetragonal columnar phase (Col$_{tet}$) at lower temperatures close to rt. Moreover, it was surprising for us that removal of a very small methoxy group from the big **PcM(OFbaC$_{60}$)(OCH$_3$)** molecule (**2** in Fig. 1) significantly lowers the cp of **C$_{12}$-PcCu(OFbaC$_{60}$)** (**3f** in Fig. 1) by about 70 $^{o}$C in comparison with that of **2** having the methoxy group [29].

In this work, we have, therefore, synthesized a homologous series of the phthalocyanine-fullerene dyads, **C$_n$-PcM(OFbaC$_{60}$)** (n=6,8,10,12; M=Cu, Ni, Co: **3a**~**f** in Scheme 1), to obtain homeotropic alignment at rt and investigate the effects of spacer chain length (n=6,8,10,12) and central metal (M=Cu, Ni, Co) on their mesomorphism. Very interestingly, each of the Pc-C$_{60}$ dyads **3a**~**e** shows perfect homeotropic alignment for the columnar mesophases at rt. Moreover, they show a unique helical structure of fullerenes around columns formed by one-dimensionally stacked Pc cores. Recently, Yoshikawa has proposed that "1D nano array structure" of donor and acceptor between two electrodes may give higher photoelectric conversion efficiency for organic thin film solar cells [30]. The present homeotropic alignment of Pc-C$_{60}$ dyads **3a**~**f** between two glass plates is the first example of the spontaneously achieved 1D nano array structure. Hence, these Pc-C$_{60}$ dyads may be very suitable to organic thin film solar cells.

We wish to report here the synthesis and spacer-chain-length effect on mesomorphic properties of the dyads **3a**~**f**, together with establishment of the very interesting helical structure of fullerenes around the Pc columns.

## 2. EXPERIMENTAL

### 2-1. Synthesis

Scheme 1 shows synthetic route of this work. The synthetic route was already developed and reported for **C$_{12}$-7**, **C$_{12}$-8**, **9f** and **3f** in our previous work [29]. In this work we have synthesized a series of the novel homologous derivatives, **C$_n$-7** (n = 6, 8, 10), **C$_n$-8** (n = 6, 8, 10), **9a**~**e** and **3a**~**e** by using the same synthetic route. The terminally

brominated *n*-alkanol derivatives **7** (**$C_n$-7**: n = 6, 8, 10, 12) were prepared from the corresponding terminally dihydroxy-substituted *n*-alkanes. The phthalonitrile derivatives **8** (**$C_n$-8**: n = 6, 8, 10, 12) were obtained from the terminally brominated *n*-alkanol derivatives **7** and commercially available 4-hydroxyphthalonitrile. Another phthalonitrile derivative, 4,5-bis(3,4-didodecyloxyphenoxy)-1,2-dicyanobenzene (**6**), was prepared by our previously reported method [26]. The phthalocyanine precursors, **$C_n$-PcCu(OH)** (**9a~f**: **a** [M = Cu, n = 6]: **b** [M = Cu, n = 8], **c** [M = Cu, n = 10] , **d** [M = Ni, n = 10] , **e** [M = Co, n = 10], **f** [M = Cu, n = 12]), were synthesized from two different phthalonitriles **6** and **$C_n$-8** in a molecular ratio of 3 : 1. The terminal OH group in **9a~f** was esterified with *p*-formyl benzoic acid by Steglich reaction [31] to afford **$C_n$-(OFba)PcM** (**10a~f**). Finally, the target Pc-$C_{60}$ dyads, **$C_n$-(OFba$C_{60}$)PcM** (**3a~f**), were synthesized from **10a~f** with N-methylglycine and fullerene by Prato reaction [32].

Since the procedures for **$C_{12}$-7**, **$C_{12}$-8**, **9f** and **3f** (n = 12) have been already reported in previous work [29], we describe here the detailed procedures only for the novel homologous derivatives, **$C_n$-7** (n = 6, 8, 10), **$C_n$-8** (n = 6, 8, 10), **9a~e** and **3a~e**.

***6-Bromo-1-hexanol**: **$C_6$-7**.*

A mixture of 1,6-hexandiol (1.25 g, 10.6 mmol), cyclohexane (20 ml) and 47% HBr aq. (20 ml) was stirred at 80 °C for 5 hrs under nitrogen atmosphere. After cooling to rt, the reaction mixture was extracted with diethyl ether and washed with water. The organic layer was dried over $Na_2SO_4$ and evaporated in *vacuo*. This crude product gave three spots ($R_f$ = 0.05, 0.43 and 0.75) on TLC (silica gel, ethyl acetate : *n*-hexane = 2 : 3). The product of Rf = 0.43 was separated by column chromatography (silica gel, ethyl acetate : *n*-hexane = 2 : 3) to afford 1.33g of 6-bromo-1-hexanol as colourless liquid. Yield: 69.3%. IR (KBr, $cm^{-1}$): 3327 (-OH), 2923 (-CH), 2852 (-CH).

***8-Bromo-1-octanol**: **$C_8$-7**.*

A mixture of 1,8-octandiol (2.50 g, 17.1 mmol), cyclohexane (38 ml) and 47% HBr aq. (38 ml) was stirred at 90 °C for 5 hrs under nitrogen atmosphere. After cooling to rt, the reaction mixture was extracted with diethyl ether and washed with water. The organic layer was dried over $Na_2SO_4$ and evaporated in *vacuo*. The residue was purified by column chromatography (silica gel, ethyl acetate : *n*-hexane = 2 : 3, $R_f$ = 0.43) to afford 0.988g of 8-bromo-1-octanol as colourless liquid. Yield: 27.6%. IR (KBr, $cm^{-1}$): 3327 (-OH), 2923 (-CH), 2852 (-CH).

***10-Bromo-1-decanol**: **$C_{10}$-7**.*

A mixture of 1,10-decandiol (2.50 g, 14.3 mmol), cyclohexane (38 ml) and 47% HBr aq. (38 ml) was stirred at 80 °C for 5 hrs under nitrogen atmosphere. After cooling to rt, the reaction mixture was extracted with n-hexane and washed with water. The organic layer was dried over $Na_2SO_4$ and evaporated in *vacuo*. The residue was purified by column chromatography (silica gel, ethyl acetate : *n*-hexane = 2 : 3, $R_f$ = 0.55) to afford 2.66g of 10-bromo-1-decanol as colourless liquid. Yield: 78.5%. IR (KBr, $cm^{-1}$): 3327 (-OH), 2923 (-CH), 2852 (-CH).

***4-(6-Hydroxyhexyloxy)phthalonitrile**: **$C_6$-8**.*

A mixture of 4-hydroxyphthalonitrile (0.25 g, 1.7 mmol), dry DMF (12 ml), potassium carbonate (0.50 g) and 6-bromo-1-hexanol **$C_6$-7** (0.41 g, 2.3 mmol) was heated at 110 °C for 1h with stirring under nitrogen atmosphere. After cooling to rt, the reaction mixture was extracted with chloroform and washed with water. The organic layer was dried over $Na_2SO_4$ and evaporated in *vacuo*. The residue was purified by column chromatography (silica gel, chloroform : THF = 4 : 1, $R_f$ = 0.58). It was recrystallized from *n*-hexane to give 0.21 g of white solid. Yield: 50%. mp 65 °C. IR (KBr, $cm^{-1}$): 3550 (OH) 2928, 2850 ($CH_2$/$CH_3$), 2226 (CN).

***4-(8-Hydroxyoctyloxy)phthalonitrile**: **$C_8$-8**.*

A mixture of 4-hydroxyphthalonitrile (0.25 g, 1.7 mmol), dry DMF (12 ml), potassium carbonate (0.50 g) and 8-bromo-1-octanol **$C_8$-7** (0.47 g, 2.3 mmol) was heated at 110 °C for 1h with stirring under nitrogen atmosphere. After

cooling to rt, the reaction mixture was extracted with chloroform and washed with water. The organic layer was dried over $Na_2SO_4$ and evaporated in *vacuo*. The residue was purified by column chromatography (silica gel, chloroform : ethyl acetate = 4 : 1, $R_f$ = 0.50). It was recrystallized from *n*-hexane to give 0.368 g of white solid. Yield: 78%. mp 61 $^oC$. IR (KBr, $cm^{-1}$): 3550 (OH) 2928, 2850 ($CH_2/CH_3$), 2226 (CN).

***4-(10-Hydoroxydecyloxy)phthalonitrile: $C_{10}$-8.***

A mixture of 4-hydroxyphthalonitrile (0.25 g, 1.7 mmol), dry DMF (12 ml), potassium carbonate (0.50 g) and 10-bromo-1-decanol **$C_{10}$-7** (0.50 ml, 2.3 mmol) was heated at 110 $^oC$ for 1h with stirring under nitrogen atmosphere. After cooling to rt, the reaction mixture was extracted with chloroform and washed with water. The organic layer was dried over $Na_2SO_4$ and evaporated in *vacuo*. The residue was purified by column chromatography (silica gel, chloroform : THF = 4 : 1, $R_f$ = 0.30). It was recrystallized from *n*-hexane to afford 0.468 g of white solid. Yield: 90%. mp 60 $^oC$. IR (KBr, $cm^{-1}$): 3550 (OH) 2928, 2850 ($CH_2/CH_3$), 2226 (CN). $^1$H-NMR ($CDCl_3$, TMS): $\delta_H$, ppm 7.70 (d, 1H, J = 8.8 Hz, Ar-*H*), 7.25 (d, 1H, J = 8.8 Hz, Ar-*H*), 7.17 (dd, 1H, $J_1$ = 8.8 Hz, $J_2$ = 2.8 Hz, Ar-*H*), 4.05 (t, 2H, J = 7.1, -OC$H_2$-), 3.67 (t, 2H, J = 7.3, -C$H_2$-), 1.89~1.81 (m, 2H, -C$H_2$-), 1.65~1.56 (m, 2H, -C$H_2$-), 1.41~1.32 (m, 12H, -C$H_2$-)

***2-(6-Hydroxyhexcyloxy)-9,10,16,17,23,24-hexakis(3,4-didodecyloxy)phthalocyaninato copper(II): $C_6$-PcCu (OH) 9a.***

A mixture of 4-(6-hydroxyhexcyloxy)phthalonitrile **$C_6$-8** (0.0500 g, 0.205 mmol) ,4,5-bis (3,4-didodecyloxyphenoxy) -1,2-dicyanobenzene **6** (0.592 g , 0.564 mmol), 1-hexanol (15 ml), DBU (8 drops) and $CuCl_2$ (55 mg, 0.41 mmol) was refluxed under nitrogen atmosphere for 24 hrs. After cooling to rt, methanol was poured into the reaction mixture to precipitate the target compound. The methanolic layer was removed by filtration. The residue was washed with methanol and acetone successively, extracted with chloroform and washed with water. The organic layer was dried over $Na_2SO_4$ and evaporated in *vacuo*. The crude product was purified by column chromatography (Silica gel, chloroform, $R_f$ = 0.38) and then recrystallized from ethyl acetate to give 0.197 g of green solid. Yield: 30.3%.

MALDI-TOF mass and elemental analysis data: See Table S1

UV-vis spectral data: See Table S2

***2-(8-Hydroxyoctyloxy)-9,10,16,17,23,24-hexakis(3,4-didodecyloxy)phthalocyaninato copper(II): $C_8$-PcCu (OH) 9b.***

A mixture of 4-(8-hydroxyoctyloxy) phthalonitrile **$C_8$-8** (0.050 g, 0.18 mmol), 4,5-bis(3,4-didodecyloxyphenoxy) -1,2-dicyanobenzene **6** (0.58 g, 0.49 mmol), 1-hexanol (18 ml), DBU (8 drops), $CuCl_2$ (0.025 g, 0.18 mmol) was refluxed under nitrogen atmosphere for 24 hrs. After cooling to rt, methanol was poured into the reaction mixture to precipitate the target compound. The methanolic layer was removed by filtration. The residue was washed with methanol and acetone successively, extracted with chloroform and washed with water. The organic layer was dried over $Na_2SO_4$ and evaporated in *vacuo*. The crude product was purified by column chromatography (Silica gel, chloroform, $R_f$ = 0.30) and then recrystallized from ethyl acetate to give 0.17 g of green solid. Yield: 30%.

MALDI-TOF mass and elemental analysis data: See Table S1

UV-vis spectral data: See Table S2

***2-(10-Hydroxydecyloxy)-9,10,16,17,23,24-hexakis(3,4-didodecyloxy)phthalocyaninato copper(II): $C_{10}$-PcCu (OH) 9c.***

A mixture of 4-(10-hydroxydecyloxy) phthalonitrile **$C_{10}$-8** (0.050 g, 0.17 mmol), 4,5-bis(3,4-didodecyloxyphenoxy) -1,2-dicyanobenzene **6** (0.48 g , 0.46 mmol), 1-hexanol (15 ml), DBU (8 drops), $CuCl_2$ (0.020 g, 0.17 mmol) was refluxed under nitrogen atmosphere for 24 hrs. After cooling to rt, methanol was poured into the reaction mixture to precipitate the target compound. The methanolic layer was removed by filtration. The residue was washed with methanol and acetone successively, extracted with chloroform and washed with water. The organic layer was dried over $Na_2SO_4$ and evaporated in *vacuo*. The crude product was purified by column chromatography (Silica gel, chloroform, $R_f$ = 0.50) and then recrystallized from ethyl acetate to give 0.16 g of green solid. Yield: 30%.

MALDI-TOF mass and elemental analysis data: See Table S1

UV-vis spectral data: See Table S2

***2-(10-Hydroxydecyloxy)-9,10,16,17,23,24-hexakis(3,4-didodecyloxy)phthalocyaninato nickel(II): $C_{10}$-PcNi (OH) 9d.***

A mixture of 4-(10-hydroxydecyloxy) phthalonitrile **$C_{10}$-8** (0.0700 g, 0.233 mmol), 4,5-bis(3,4-didodecyloxyphenoxy) -1,2-dicyanobenzene **6** (0.673 g , 0.641 mmol), 1-hexanol (20 ml), DBU (4 drops), $NiCl_2$ (0.0604 g, 0.466 mmol) was refluxed under nitrogen atmosphere for 24 hrs. After cooling to rt, methanol was poured into the reaction mixture to precipitate the target compound. The methanolic layer was removed by filtration. The residue was washed with methanol and acetone successively, extracted with chloroform and washed with water. The organic layer was dried over $Na_2SO_4$ and evaporated in *vacuo*. The crude product was purified by column chromatography (Silica gel, chloroform, $R_f$ = 0.83) and then recrystallized from ethyl acetate to give 0.130 g of green solid. Yield: 17.3%.

MALDI-TOF Mass and Elemental Analysis data: See Table S1

UV-vis spectral data: See Table S2

***2-(10-Hydroxydecyloxy)-9,10,16,17,23,24-hexakis(3,4-didodecyloxy)phthalocyaninato cobalt(II): $C_{10}$-PcCo(OH) 9e.***

A mixture of 4-(10-hydroxydecyloxy) phthalonitrile **$C_{10}$-8** (0.0500 g, 0.170 mmol), 4,5-bis(3,4-didodecyloxyphenoxy) -1,2-dicyanobenzene **6** (0.500 g , 0.467 mmol), 1-hexanol (18 ml), DBU (4 drops), $CoCl_2 \cdot 6H_2O$ (0.0931 g, 0.340 mmol) was refluxed under nitrogen atmosphere for 24 hrs. After cooling to rt, methanol was poured into the reaction mixture to precipitate the target compound. The methanolic layer was removed by filtration. The residue was washed with methanol and acetone successively, extracted with chloroform and washed with water. The organic layer was dried over $Na_2SO_4$ and evaporated in *vacuo*. The crude product was purified by column chromatography (Silica gel, chloroform, $R_f$ = 0.50) and then recrystallized from ethyl acetate to give 0.0859 g of green solid. Yield: 15.4%.

MALDI-TOF Mass and Elemental Analysis data: See Table S1

UV-vis spectral data: See Table S2

***Copper benzoic derivative: $C_6$-PcCu(OFba) 10a.***

A mixture of **$C_6$-PcCu(OH) 9a** (139 mg, 0.0402 mmol), p-formyl benzoic acid (12.1 mg, 0.0804 mmol), dry $CH_2Cl_2$ (15 ml), N,N'-dicyclohexylcarbodiimide (82.9 mg, 0.402 mmol), N,N-dimethyl-4-aminopyridine (19.6 mg, 0.161 mmol) was stirred at rt under nitrogen atmosphere for 30 h. The reaction mixture was extracted with chloroform and washed with water. The organic layer was dried over $Na_2SO_4$ and evaporated in *vacuo*. The residue was purified by column chromatography (silica gel, chloroform, $R_f$ = 0.88) and then recrystallized from ethyl acetate to 137 mg of give green solid. Yield: 95.1%.

MALDI-TOF mass and elemental analysis data: See Table S1

UV-vis spectral data: See Table S2

***Copper benzoic derivative: $C_8$-PcCu(OFba) 10b.***

A mixture of **$C_8$-PcCu(OH) 9b** (100 mg, 0.0287 mmol), p-formyl benzoic acid (8.60 mg, 0.0574 mmol), dry $CH_2Cl_2$ (15 ml), N,N'-dicyclohexylcarbodiimide (59.2 mg, 0.287 mmol), N,N-dimethyl-4-aminopyridine (14.0 mg, 0.115 mmol) was stirred at rt under nitrogen atmosphere for 30 h. The reaction mixture was extracted with chloroform and washed with water. The organic layer was dried over $Na_2SO_4$ and evaporated in *vacuo*. The residue was purified by column chromatography (silica gel, chloroform, $R_f$ = 1.0) and then recrystallized from ethyl acetate to 65.6 mg of give green solid. Yield: 63.1%.

MALDI-TOF mass and elemental analysis data: See Table S1

UV-vis spectral data: See Table S2

***Copper benzoic derivative: $C_{10}$-PcCu(OFba) 10c.***

A mixture of **$C_{10}$-PcCu(OH) 9c** (100 mg, 0.0285 mmol), *p*-formyl benzoic acid (8.56 mg, 0.0570 mmol), dry $CH_2Cl_2$ (15 ml), N,N'-dicyclohexylcarbodiimide (59.0 mg, 0.285 mmol), N,N-dimethyl-4-aminopyridine (14.0 mg, 0.114 mmol) was stirred at rt under nitrogen atmosphere for 30 h. The reaction mixture was extracted with chloroform and washed with water. The organic layer was dried over $Na_2SO_4$ and evaporated in *vacuo*. The residue was purified by column chromatography (silica gel, chloroform, $R_f$ = 0.88) and then recrystallized from ethyl acetate to 53.9 mg of give green solid. Yield: 57.0%.

MALDI-TOF mass and elemental analysis data: See Table S1

UV-vis spectral data: See Table S2

***Nickel benzoic derivative: $C_{10}$-PcNi(OFba) 10d.***

A mixture of **$C_{10}$-PcNi(OH) 9d** (80.4 mg, 0.0229 mmol), *p*-formyl benzoic acid (6.88 mg, 0.0458 mmol), dry $CH_2Cl_2$ (15 ml), N,N'-dicyclohexylcarbodiimide (47.2 mg, 0.229 mmol), N,N-dimethyl-4-aminopyridine (11.2 mg, 0.0916 mmol) was stirred at rt under nitrogen atmosphere for 23 h. The reaction mixture was extracted with chloroform and washed with water. The organic layer was dried over $Na_2SO_4$ and evaporated in *vacuo*. The residue was purified by column chromatography (silica gel, chloroform, $R_f$ = 0.93) and then recrystallized from ethyl acetate to 75.3 mg of give green solid. Yield: 90.3%.

MALDI-TOF Mass and Elemental Analysis data: See Table S1

UV-vis spectral data: See Table S2

***Cobalt benzoic derivative: $C_{10}$-PcCo(OFba) 10e.***

A mixture of **$C_{10}$-PcCo(OH) 9e** (76.5 mg, 0.0218 mmol), *p*-formyl benzoic acid (6.55 mg, 0.0436 mmol), dry $CH_2Cl_2$ (15 ml), N,N'-dicyclohexylcarbodiimide (45.0 mg, 0.218 mmol), N,N-dimethyl-4-aminopyridine (10.7 mg, 0.0872 mmol) was stirred at rt under nitrogen atmosphere for 23 h. The reaction mixture was extracted with chloroform and washed with water. The organic layer was dried over $Na_2SO_4$ and evaporated in *vacuo*. The residue was purified by column chromatography (silica gel, chloroform, $R_f$ = 1.00) and then recrystallized from ethyl acetate to 61.2 mg of give green solid. Yield: 77.1%.

MALDI-TOF Mass and Elemental Analysis data: See Table S1

UV-vis spectral data: See Table S2

***Copper fullerene derivative: $C_6$-PcCu(OFba$C_{60}$) 3a.***

A mixture of **$C_6$-PcCu(OFba) 10a** (170 mg, 0.0473 mmol), $C_{60}$ fullerene (68.1 mg, 0.0946 mmol), *N*-methylglycine (10.1 mg, 0.114 mmol ), dry toluene (50 ml) was refluxed under $N_2$ for 12 h. After cooling to rt, the reaction mixture was extracted with chloroform and washed with water. The organic layer was dried over $Na_2SO_4$ and evaporated in *vacuo*. Unreacted fullerene was removed by flash chromatography (silica gel, n-hexane : chloroform = 1 : 1, $R_f$ = 1.0) and the residue in silica gel was flushed out with chloroform. The crude product was recrystallized from ethyl acetate to obtain 192 mg of green solid. Yield: 93.7%.

MALDI-TOF mass and elemental analysis data: See Table S1

UV-vis spectral data: See Table S2

***Copper fullerene derivative: $C_8$-PcCu(OFba$C_{60}$) 3b.***

A mixture of **$C_8$-PcCu(OFba) 10b** (50.0 mg, 0.0138 mmol), $C_{60}$ fullerene (19.9 mg, 0.0276 mmol), N-methylglycine (2.95 mg 0.0331 mmol), dry toluene (50 ml) was s refluxed under $N_2$ for 10 h. After cooling to rt, the reaction mixture was extracted with chloroform and washed with water. The organic layer was dried over $Na_2SO_4$ and evaporated in *vacuo*. Unreacted fullerene was removed by flash chromatography (silica gel, toluene, $R_f$ = 1.0) and the residue in silica

gel was flushed out with THF. The crude product was recrystallized from ethyl acetate to obtain 46.2 mg of green solid. Yield: 76.7%.

MALDI-TOF mass and elemental analysis data: See Table S1

UV-vis spectral data: See Table S2

***Copper fullerene derivative: $C_{10}$-PcCu(OFba$C_{60}$) 3c.***

A mixture of **$C_{10}$-PcCu(OFba) 10c** (50.0 mg, 0.0137 mmol), $C_{60}$ fullerene (19.7 mg, 0.0274 mmol), N-methylglycine (2.93 mg, 0.0329 mmol), dry toluene (50 ml) was refluxed under $N_2$ for 12 h. After cooling to rt, the reaction mixture was extracted with chloroform and washed with water. The organic layer was dried over $Na_2SO_4$ and evaporated in *vacuo*. Unreacted fullerene was removed by flash chromatography (silica gel, toluene, $R_f$ = 1.0) and the residue in silica gel was flushed out with THF. The crude product was recrystallized from ethyl acetate to obtain 52.0 mg of green solid. Yield: 86.2%.

MALDI-TOF mass and elemental analysis data: See Table S1

UV-vis spectral data: See Table S2

***Nickel fullerene derivative: $C_{10}$-PcNi(OFba$C_{60}$) 3d.***

A mixture of **$C_{10}$-PcNi(OFba) 10d** (60.0 mg, 0.0165 mmol), $C_{60}$ fullerene (23.8 mg, 0.0330 mmol), N-methylglycine (3.5 mg, 0.040 mmol), dry toluene (45 ml) was refluxed under $N_2$ for 12 h. After cooling to rt, the reaction mixture was extracted with chloroform and washed with water. The organic layer was dried over $Na_2SO_4$ and evaporated in *vacuo*. Unreacted fullerene was removed by flash chromatography (silica gel, toluene, $R_f$ = 1.0) and the residue in silica gel was flushed out with chloroform. The crude product was recrystallized from ethyl acetate to obtain 64.8 mg of green solid. Yield: 89.5%.

MALDI-TOF Mass and Elemental Analysis data: See Table S1

UV-vis spectral data: See Table S2

***Cobalt fullerene derivative: $C_{10}$-PcCo(OFba$C_{60}$) 3e.***

A mixture of **$C_{10}$-PcCo(OFba) 10e** (38.0 mg, 0.0104 mmol), $C_{60}$ fullerene (15.0 mg, 0.0208 mmol), N-methylglycine (2.23 mg, 0.0250 mmol), dry toluene (30 ml) was refluxed under $N_2$ for 12 h. After cooling to rt, the reaction mixture was extracted with chloroform and washed with water. The organic layer was dried over $Na_2SO_4$ and evaporated in *vacuo*. Unreacted fullerene was removed by flash chromatography (silica gel, toluene, $R_f$ = 1.0) and the residue in silica gel was flushed out with a mixture solvent (*n*-hexane : chloroform = 1 : 1). The crude product was recrystallized from ethyl acetate to obtain 35.3 mg of green solid. Yield: 77.4%.

MALDI-TOF Mass and Elemental Analysis data: See Table S1

UV-vis spectral data: See Table S2

**2-2. Measurements**

The Infrared absorption spectra were recorded by using a Nicolet NEXUS670 FT-IR. The $^1$H-NMR measurements were carried out by using $^1$H-NMR (Bruker Ultrashield 400 M Hz). The elemental analyses were performed by using a Perkin-Elmer Elemental Analyzer 2400. The MALDI-TOF mass spectral measurements were carried out by using a Bruker Daltonics Autoflex III spectrometer (matrix: dithranol). Temperature-dependent electronic absorption (UV-vis) spectra were recorded by using a Hitachi U-4100 spectrophotometer equipped with a hand-made temperature controller [33]. Phase transition behaviour of the present compounds was observed with polarizing optical microscope (Nikon ECLIPSE E600 POL) equipped with a Mettler FP82HT hot stage and a Mettler FP-90 Central Processor, and a Shimadzu DSC-50 differential scanning calorimeter. The mesophases were identified by using a wide angle X-ray

diffractometer (Rigaku Rad) with Cu-Kα radiation and a hand-made hot stage equipped with a temperature controller [33], and a small angle X-ray diffractometer (Bruker Mac SAXS System) equipped with a temperature-variable sample holder adopted a Mettler FP82HT hot stage. Figs. S1 and S2 illustrate the setup of the SAXS system and the setup of the temperature-variable sample holder, respectively. As can be seen from Fig. S1, the generated X-ray is bent by two convergence monochrometers to produce point X-ray beam (diameter = 1.0 mm). The point beam runs through holes of the temperature-variable sample holder. As illustrated in Fig. S2, into the temperature-variable sample holder of Mettler FP82HT hot stage, a glass plate (76 mm × 19 mm × 1.0 mm) having a hole (diameter = 1.5 mm) is inserted. The hole can be charged with a powder sample (*ca.* 1 mg). The measurable range is from 3.0 Å to 100 Å and the temperature range is from rt to 375 °C. This SAXS system is available for all condensed phases including fluid nematic phase and isotropic liquid.

## 3. RESULTS AND DISCUSSION

### 3-1. Synthesis of Pc precursors and Pc-$C_{60}$ dyads

In Table S1 are summarized MALDI-TOF mass spectral data, elemental analysis data, and yields of **9a**~**f**, **10a**~**f**, and **3a**~**f**. The Pc precursors, **$C_n$-PcCu(OH)** (**9a**~**f**), were obtained in yields of 15-30%. These low yields are attributed to the undesirable **(4:0)PcCu** by-products which are composed of only four 4,5-bis(3,4-didodecyloxyphenoxy)-1,2-dicyanobenzene (**6** in Scheme 1) units. On the other hand, the intermediate Pc precursors, **$C_n$-PcCu(OFba)** (**10a**~**f**), and the final target Pc-$C_{60}$ dyads, **$C_n$-PcM(OFba$C_{60}$)** (**3a**~**f**), could be synthesized in good yields by Steglich esterification reaction [31] and Prato reaction [32], respectively.

As can be seen from Table S1, the Pc derivatives **9a**~**f** and **10a**~**f** gave satisfactory elemental analysis data. On the other hand, elemental analysis of the Pc-$C_{60}$ dyads **3f** synthesized in our previous work was also carried out, but it was not completely burnt out that the observed carbon content showed lower percentage than the calculated value by several percent [29]. This is a well-known characteristic of less flammable phthalocyanine derivatives [34]. Hence, we did not furthermore carry out the elemental analyses for other Pc-$C_{60}$ dyads **3a~e** and the results of the elemental analyses are omitted here for **3a**~**f**. However, the MALDI-TOF mass and electronic spectra listed in Tables S1 and S2 gave satisfactory evidences of successful syntheses of the target Pc-$C_{60}$ dyads **3a**~**f**, as mentioned below.

As can be seen from Table S1, the observed values and the calculated value of mass for **$C_6$-PcCu(OFba$C_{60}$)** (**3a**), for example, are (4336.89, 3616.64) and 4337.54, respectively. The observed values gave two peaks for all the **$C_n$-PcM(OFba$C_{60}$)** (**3a~f**) dyads. One peak corresponds to the calculated molecular weight. On the other hand, another peak corresponds to a molecular weight smaller by about 720 than the calculated molecular weight. The mass of 720 is compatible with the molecular weight of fullerene($C_{60}$). The fraction peak smaller by 720 than the calculated value may be resulted from cleavage of the fullerene ($C_{60}$) moiety from the **$C_n$-PcM(OFba$C_{60}$)** (**3a~f**) dyads by the laser irradiation in the MALDI-TOF mass measurements.

To further confirm the formation of these Pc-$C_{60}$ dyads, electronic absorption spectra were measured for the chloroform solutions of the **$C_n$-PcM(OFba$C_{60}$)** (**3a~f**) dyads. The electronic spectral data are summarized in Table S2. An absorption characteristic to fullerene appears at *ca.* 250 nm in the electronic spectra [35]. As can be seem from this table, each of the **$C_n$-PcM(OFba$C_{60}$)** (**3a~f**) dyads gave an additional peak at *ca.* 246~256 nm characteristic to fullerene moiety. The **$C_n$-PcCu(OFba)** (**10a~f**) precursors did not give such an additional peak at *ca.* 246~256 nm. From these

electronic spectral data, it was also certified that each of the **$C_n$-PcM(OFbaC$_{60}$)** (**3a~f**) derivatives bears a fullerene moiety.

Although we tried to measure $^1$H NMR spectra of the diamagnetic PcNi derivatives, **9d**, **10d** and **3d**, all our attempts were in vain. As is well-known, phthalocyanine discotic liquid crystals tend to aggregate even in a very dilute chloroform solution like as $10^{-6}$ M. We could not measure $^1$H NMR spectra for such a dilute solution. So, we need to increase the concentration to ca. $10^{-3}$ M for the NMR measurements. However, very strong aggregation took place in such a concentrated solution, and it always gave the very broad meaningless NMR spectra. However, as mentioned above we confirmed from MALDI-TOF mass spectra and the UV-vis spectra that all the target Pc-fullerene dyads, **$C_n$-PcM(OFbaC$_{60}$)** (**3a~f**), could be successfully synthesized.

### 3-2. Phase transition behaviour

Table 1 summarises phase transition behaviour of **$C_n$-PcCu(OH)** (**9a~f**), **$C_n$-PcCu(OFba)** (**10a~f**) and **$C_n$-PcM(OFbaC$_{60}$)** (**3a~f**). Tables S3, S4 and S5 list up X-ray data of **9a~f**, **10a~f** and **3a~f**, respectively. Phase transition behaviour of these compounds was established by using polarizing microscopy (POM), differential scanning calorimeter (DSC), and temperature-dependent wide and small angle X-ray diffractometers (WAXS and SAXS).

***Precursors 9a~f and 10a~f***

As you can be seen from Table 1, each of the phthalocyanine (Pc) precursors, **9a~f** and **10a~f**, shows plural columnar mesophases. Interestingly, the shorter-spacer-substituted Pc precursors tend to show hexagonal columnar ($Col_h$) mesophases, whereas the longer-spacer-substituted Pc precursors tend to show tetragonal columnar ($Col_{tet}$) mesophases and a bicontinuous cubic (Cub(Pn3m)) mesophase.

***Pc-fullerene dyads 3a~f***

As you can be seen from Table 1, it is very interesting that the Pc-fullerene dyads **3a~f** also show the same tendency: the shorter-spacer-substituted dyads **3a**,**b** (n = 6, 8; M = Cu) showed a $Col_h$ mesophase, whereas the longer-spacer-substituted dyads **3c~f** (n = 10, 12; M = Cu, Ni, Co) showed a $Col_{tet}$ mesophase.

Each of the freshly prepared dyads **3a~f** is a crystalline sate at rt. When the crystal was heated, it gradually transformed into an **ordered** columnar mesophase, $Col_{ho}$ for **3a**,**b** (n = 6, 8; M = Cu) or $Col_{tet.o}$ for **3c~f** (n = 10, 12; M = Cu, Ni, Co), exhibiting a perfect homeotropic alignment at the same time. Once it was heated up over the clearing point (cp) and then the resulted isotropic liquid was cooled down to rt, it transformed into a **disordered** columnar mesophase, $Col_{hd}$ for **3a**,**b** or $Col_{tet.d}$ for **3c~e**, exhibiting a perfect homeotropic alignment. Gradual decomposition was observed only for **3f** in several heating and cooling cycles, and small birefringent spots gradually appeared and increased in the homeotropically aligned dark area of the $Col_{tet.d}$ mesophase. Hence, Table 1 omits the $Col_{tet.d}$ mesophase in cooling stage for **3f**. The homeotropic alignment of $Col_{hd}$ and $Col_{tet.d}$ was very stable and did not change at rt for several months.

Fig. 2 shows photomicrographs of perfect homeotropic alignment for a casted thin film of the representative Pc-$C_{60}$ dyad, **$C_{10}$-PcCu(OFbaC$_{60}$)** (**3c**), at 80 $^o$C, together with their columnar alignment models. As can be seen from the left photomicrograph in this figure, the casted film was completely dark between cross polaraizers. The scrached part in the right photomicrograph showed birefringence. This means that perfect homeotropic alignment was achieved in the left photomicrograph but that the homeotropically aligned columns in the right photomicrograph were disturbed by scratching, as illustrated the columnar alignment model in the bottom of this figure. The present homeotropic alignment is very favourable for solar cell fabrication [25, 29, 30]. Furthermore, the present Pc-$C_{60}$ dyads (**3a~f**) show very simple phase transition, in comparison with the Pc precursors (**9a~f** and **10a~f**). No phase transition of the non-virgin sample may be very suitable for organic thin film solar cells, because the stable performance can be achieved without any phase transitions at all temperatures.

### 3-3. Mesophase appearance depending on the spacer chain length between Pc and fullerene

As mentioned above, very interestingly, the shorter-spacer-substituted dyads **3a**,**b** (n = 6, 8; M = Cu) showed a $Col_h$ mesophase, whereas the longer-spacer-substituted dyads **3c**~**f** (n = 10, 12; M = Cu, Ni, Co) showed a $Col_{tet}$ mesophase. Thus, appearance of the mesophase depends not on the central metal but on the spacer chain length between Pc and fullerene. Fig. 3 illustrates the possible origin of formation of $Col_h$ and $Col_{tet}$ mesophases depending on the spacer length. It may be attributable to freedom of rotation of the dyad, taking our previous work [36] into consideration. As illustrated in this figure, the columns formed by the shorter-spacer-substituted dyads **3a**,**b** (n = 6, 8; M = Cu) can freely rotate to show a $Col_h$ mesophase. On the other hand, the columns formed by the longer-spacer-substituted dyads **3c**~**f** (n = 10, 12; M = Cu, Ni, Co) cannot freely rotate but the rotation may be restricted by confliction of prominent fullerenes to show a $Col_{tet}$ mesophase. This may become a very interesting new guideline to control the mesophase for dyads.

### 3-4. Temperature dependent small angle X-ray diffraction patterns

In this study, we carried out at the first time temperature-dependent small angle X-ray (SAXS) diffraction measurements for all the Pc precursors (**9a**~**f** and **10a**~**f**) and the Pc-$C_{60}$ dyads (**3a**~**f**). Fig. 4 shows the SAXS patterns of the representative compounds, **$C_8$-PcCu(OH)** (**9b**), **$C_8$-PcCu(OFba)** (**10b**) and **$C_8$-PcCu(OFba$C_{60}$)** (**10b**), together with a previous symmetrical (4:0) derivative, **(4:0)PcCu**, which is composed of only four 4,5-bis(3,4-didodecyloxyphenoxy)-1,2-dicyanobenzene units (**6**) [9].

As can be seen from this figure, the symmetrical derivative, **(4:0)PcCu**, did not give any reflection peaks in very small angle region of $0.8 < 2\theta < 2.0$ degree (Fig. 4[A]). On the other hand, an additional peak appeared in this region for all the present asymmetrical (3:1) compounds, **$C_8$-PcCu(OH)** (**9b**), **$C_8$-PcCu(OFba)** (**10b**) and **$C_8$-PcCu(OFba$C_{60}$)** (**3b**). The Pc precursors **$C_8$-PcCu(OH)** (**9b**) and **$C_8$-PcCu(OFba)** (**10b**) gave a relatively small additional peak in this region for lower temperature phases (Fig. 4[B] and [C]), whereas the Pc-$C_{60}$ dyads **$C_8$-PcCu(OFba$C_{60}$)** (**3b**) gave a very big peak for K and $Col_{ho}$ phases and a shoulder even for the isotropic liquid (IL) in this small angle region (Fig. 4[D]). As can be seen from Fig. S3 and Table S4, each of the Pc-$C_{60}$ dyads **$C_n$-PcM(OFba$C_{60}$)** (**3a~f** for n = 6, 8, 10, 12; M = Cu, Ni, Co) gave the big additional peak in the small angle region, irrespective of spacer length and central metal. The big additional peak may be originated from the substituent bulkiness of fullerene.

Very interestingly, this additional peak could not be indexed to any reflections from the 2D lattices of all the columnar mesophases reported up to date. Therefore, we denote this additional unique peak as Peak H, hereafter.

### 3-5. Clarification of Peak H by temperature dependent small angle X-ray diffraction studies

Hereupon, we wanted to clarify the origin of the peak H by using temperature dependent small angle X-ray diffraction (SAXS) techniques. As illustrated in Fig. 5, we have three different alignments of liquid crystalline columns for SAXS measurements: [A] non-aligned sample (for Polydomain Method = powder method for X-ray crystal analysis), [B] *homogeneously* aligned sample (for Monodomain Method 1), and [C] *homeotropically* aligned sample (for Monodomain Method 2).

Until now, we have adopted only Polydomain Method for non-aligned sample, as illustrated in Fig. 5 [A] and Fig. S2. For this method, polydomain of liquid crystalline paste is filled into a hole of glass plate. In this case, both the reflections from two-dimensional and one-dimensional lattices can be observed separately, as illustrated in Fig. 5 [A]. The small and large rings correspond to reflections from a two-dimensional lattice (in XY plane) and a one-dimensional lattice (in Z-direction), respectively. On the other hand, the homogeneously aligned samples give only a reflection from one-dimensional lattice as a large ring (Fig. 5[B]), which corresponds to the stacking periodicity in Z-direction of columns;

the homeotropically aligned samples give only reflections from two-dimensional lattice in XY plane as small rings (Fig. 5[C]).

As mentioned above, each of the Pc-$C_{60}$ dyads **3a~f** shows perfect homeotropic alignment between two glass plates. If the peak H would be a periodicity along the Z axis direction of column, the peak H should disappear for the homeotropically aligned sample, as the same case as Fig. 5[C]. Therefore, we prepared a homeotropically aligned sample with PET film spacer (50 μm thickness) intervened between two cover glass plates (18mm × 18 mm × 0.12~0.17mm). The freshly synthesised Pc-$C_{60}$ dyads (**3c~e**) were used for this SAXS samples and annealed at 90 °C(**3c**) or 95 °C(**3e**,**d**) for one hour to achieve perfect homeotropic alignment between two cover glass plates.

As shown in Fig. 6, both Peak H and (100) reflection peak could be clearly observed for all the non-aligned samples, whereas Peak H only disappeared for all the homeotropically aligned samples of **3c~e**. This means that Peak H is a periodicity along the Z axis direction of column. As already mentioned, Peak H could not be indexed to any reflections from the 2D lattices in XY plane of all the columnar mesophases reported up to date, and moreover Peak H may be originated from the substituent of fullerene.

### 3-6. Helical structure of fullerenes around Pc core columns

From these results, we propose a columnar structure model, as illustrated for a representative Pc-$C_{60}$, dyad **$C_{10}$-PcCu(OFbaC$_{60}$)** (**3c**), in Fig. 7. As can be seen from Fig. 7[A], the stacking distance among Pc disks in the columns is 4.84 Å, in which about 10 Å of fullerene balls cannot be inserted. Therefore, fullerene balls should exist outside in a fan-like area of the less alkyl chains. The less-density of fan-shaped area may rotate so as to average the density in column with avoiding steric hindrance of the bulky fullerenes, as illustrated in Fig. 7[B]. Moreover, fullerenes tend to so strongly aggregate that they may adjoin each other to pile up in helical fashion, as illustrated in Fig. 7[C]. Therefore, Peak H should correspond to the helical pitch (74.4 Å). It is consistent with the periodicity along the Z axis direction of column that was clarified from SAXS monodomain method, as mentioned above. When the helical pitch of fullerenes (74.4 Å) is divided by the stacking distance of Pc disks (4.84 Å), we can estimate the number of the Pc-$C_{60}$ dyads in a pitch to be about sixteen and 23.4° for the rotation angle of the dyads. At this present time, we could not determine whether the helicity of fullerenes is right-handed or left-handed by using circular dichroism spectroscopy, because the intensity was too weak to be distinguishable. Hence, it may be a racemic mixture. Further studies are needed using a new homologue substituted by chiral alky chains. Nevertheless, to our best knowledge, this is the first established example of the helical structure of fullerenes in columnar liquid crystalline donor-acceptor dyads [13-25].

## 4. CONCLUSION

In this study, we have synthesised a homologous series of columnar liquid crystalline donor-acceptor type of phthalocyanine-fullerene dyads, **$C_n$-PcM(OFbaC$_{60}$)** (n = 6, 8, 10, 12; M = Cu, Ni, Co: **3a~f**), together with their phthalocyanine precursors, **$C_n$-PcCu(OH)** (**9a~f**) and **$C_n$-PcCu(OFba)** (**10a~f**), and established their mesomorphism.

Interestingly, the shorter-spacer-substituted (n = 6, 8; M = Cu) dyads **3a**,**b** showed a hexagonal columnar mesophase ($Col_h$), whereas the longer-spacer-substituted (n = 10, 12; M = Cu, Ni, Co) dyads **3c~f** showed a tetragonal columnar mesophase ($Col_{tet}$). Moreover, each of the Pc-$C_{60}$ dyads, **$C_n$-PcM(OFbaC$_{60}$)** (**3a~e**), shows perfect homeotropic alignment in both the $Col_h$ and $Col_{tet}$ mesophases at rt. More interestingly, these columnar mesophases gave a very unique XRD reflection peak denoted as Peak H in a very small angle region of $0.8 < 2\theta < 2.0$ degree. We have established at the first time from our developed two new XRD sample preparation techniques that the Peak H is due to the helical structure of fullerenes around columns formed by one-dimensionally stacked Pc cores. The present

homeotropic alignment of Pc-$C_{60}$ dyads **3a**~**f** between two glass plates is the first example of the spontaneously achieved 1D nano array structure of donor-acceptor dyads, so far as we know. Hence, these Pc-$C_{60}$ dyads may be very suitable to organic thin film solar cells.

**Acknowledgement**

This work is partially supported by Grant-in-Aid for science research (Grant No. 2236012311) from the Ministry of Education, Culture, Sports, Science and Technology, Japan. We are also deeply grateful to Associate Prof. Yoichi Takanishi, Kyoto University for his valuable suggestion on Monodomain Method for our SAXS sample preparation.

## REFERENCES

1. Kim JY, Bard AJ. *Chem. Phys. Lett.* 2004; **383**: 11–15.
2. Nishizawa T, Tajima K, Hashimoto K. *J. Mater. Chem.* 2007; **17**: 2440–2445.
3. Roland T, Ramirez GH, Léonard J, Méry S, Haacke S. *J. Phys.: Conference Series* 2011; **276**: 012006(1-6).
4. Lincker F, Heinrich B, Bettignies R, Rannou P, Pecaut J, Grevin B, Pron A, Donnio B, Demadrille R. *J. Mater. Chem.* 2011; **21**: 5238-5247.
5. Barrau S, Heiser T, Richard F, Brochon C, Ngov C, van de Wetering K, Hadziioannou G, Anokhin DV, Ivanov DA. *Macromolecules*. 2008; **41**: 2701-2710.
6. Kim DH, Lee BL, Moon H, Kang HM, Jeong EJ, Park JI, Han KM, Lee S, Yoo BW, Koo BW, Kim JY, Lee YH, Cho K, Becerril HA, Bao Z. *J. Am. Chem. Soc.* 2009; **131**: 6124-6132.
7. Liang TC, Chiang IH, Yang PJ, Kekuda D, Chu CW, Lin HC. *J. Poly. Sci.: Part A Poly. Chem.* 2009; **47**: 5998-6013
8. Sommer M, Huettner S, Thelakkat M. *J. Mater. Chem.* 2010; **20**; 10788–10797.
9. Yao K, Chen Y, Chen L, Li F, Li X, Ren X, Wang H, Liu T. *Macromolecules*. 2011; **44**: 2698–2706.
10. Yasuda T, Yonezawa K, Ito M, Kamioka H, Han L, Moritomo Y. *J. Photopolym. Sci. Technol.* 2012; **25**: 271-276.
11. Han Y, Chen L, Chen Y. *J. Poly. Sci. Poly. Chem.* 2012; published online: DOI: 10.1002/pola.26394.
12. Li F, Chen W, Chen Y. *J. Mater. Chem.* 2012; **22**: 6259-6266.
13. Bushby JR, Hamley IW, Liu Q, Lozman OR, Lydon EJ. *J Mater Chem.* 2005; **15**: 4429-4434.
14. Uchida S, Kude Y, Nishikitani Y, Ota (= Ohta) K. *Jpn. Kokai Tokkyo Koho.* JP 2008214227(A)-2008-09-18 (Priority number: JP2007060604; Submission Date: 2007-03-09)
15. Zhou X, Kang SW, Kumar S, Kulkarni RR, Cheng SZD, Li Q. *Chem. Mater*, 2011; **20**: 3551-3553.
16. de la Escosura A, Martınez-Dıaz MV, Barbera J, Torres T. *J. Org. Chem*., **2008**; 73; 1475-1480.
17. Tashiro K, Aida T. *J Amer. Chem. Soc.* 2008; **130** ; 13812–13813.
18. Geerts YH, Debever O, Amato C, Sergeyev S. *Beilstein J. Org. Chem.* 2009; **5**, 1-9.
19. Thiebaut O, Bock H, Grelet E. *J. Am. Chem. Soc.* 2010; **132**: 6886–6887.
20. Hayashi H, Nihashi W, Umeyama T, Matano Y, Seki S, Shimizu Y, Imahori H. *J. Am. Chem. Soc.* 2011; **133** : 10736–10739.
21. Bagui M, Dutta T, Chakraborty S, Melinger JS, Zhong H, Keightley A, Peng Z. *J. Phys. Chem. A* 2011; **115**: 1579–1592.
22. Haverkate LA, Zbiri M, Johnson MR, Deme B, de Groot HJM, Lefeber F, Kotlewski A, Picken SJ, Mulder FM, Kearley GJ. *J. Phys. Chem. B* 2012; **116**: 13098-13105.

23. Ota (= Ohta) K. *Jpn. Kokai Tokkyo Koho*, JP2011132180(A)-2011-07-07 (Priority number: JP20090293501; Submission Date: 2009-12-24).
24. Ince M, Martinez-Diaz MV, Barbera, J, Torres, T. *J. Mater. Chem.* 2011; **21**: 1531-1536.
25. Kamei T, Kato T, Itoh E, Ohta K. *J. Porphyrins Phthalocyanines* 2012; **16**: 1261–1275.
26. Hatsusaka K, Ohta K, Yamamoto I and Shirai H. *J. Mater. Chem.* 2001; **11**: 423–433.
27. Bingel C. *Chem. Ber.* 1993; **126**: 1957-1959.
28. Maggini M, Scorrano G, Prato M. *J. Am. Chem. Soc.* 1993; **115**: 9798-9799.
29. Shimizu M, Tauchi L, Nakagaki T, Ishikawa A, Itoh E, Ohta K. *J. Porphyrins Phthalocyanines* 2013, in press.
30. Yoshikawa S. "Supra-hierarchical Nano-structured Organic Thin Film Solar Cells," JST-DFG Joint WS <http://www.jst.go.jp/sicp/ws2009_ge3rd/ abstract/20.pdf>.
31. Neises B, Steglish W. *Angew. Chem. Int. Ed.* 1978; **17**: 522- 524.
32. Maggini M, Scorrano G, Prato M. *J. Am. Chem. Soc.*, 1993; **115**: 9798-9799.
33. Hasebe H. *Master Thesis,* Sinshu University (1991); Ema H. *Master Thesis*, Sinshu University (1988).
34. van der Pol JF, Neeleman E, van Miltenburg JC, Zwikker JW, Nolte RJM and Drenth W. *Macromolecules* 1990; **23**: 155–162.
35. Sastre A, Gouloumis A, Vazquez P, Torres T, Doan V, Schwartz BJ, Wudl F, Euhegoyen L and Rivera J. *Org. Lett.* 1999; **1**: 1807–1810.
36. Komatsu T, Ohta K, Watanabe T, Ikemoto H, Fujimoto T, Yamamoto I. *J. Mater. Chem.* 1994: **4**; 537-540.

## (A) Previous work using Bingel reaction

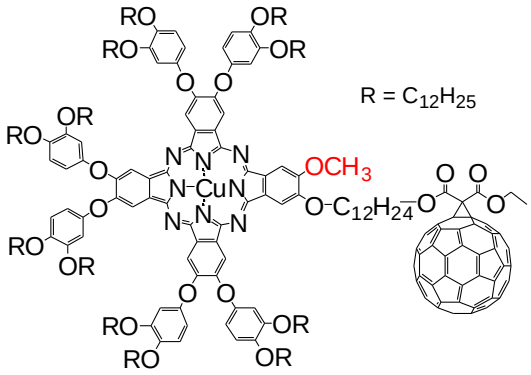


**PcCu(OMalC$_{60}$)(OCH$_3$): 1**

## (B) Previous work using Prato reaction

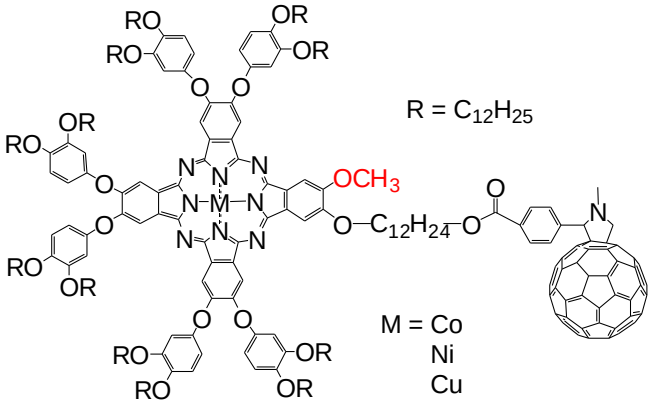


**PcM(OFbaC$_{60}$)(OCH$_3$): 2**

## (C) This work using Prato reaction without methoxy group

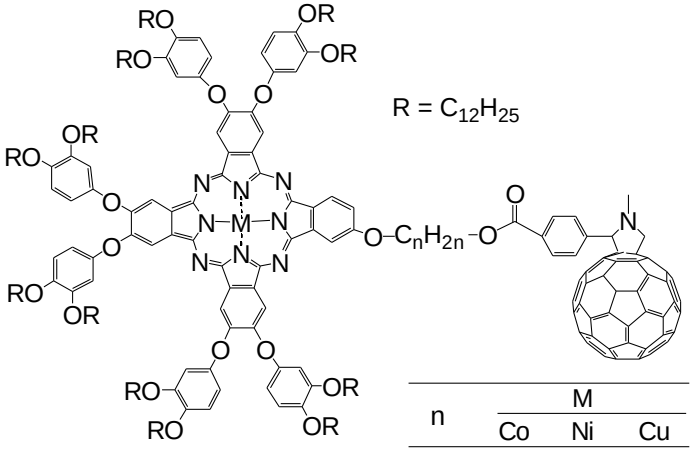


**C$_n$-PcM(OFbaC$_{60}$): 3**

| n | M | | |
|---|---|---|---|
| | Co | Ni | Cu |
| 6 | - | - | **a** |
| 8 | - | - | **b** |
| 10 | **e** | **d** | **c** |
| 12 | - | - | **f*** |

**Fig. 1** Molecular formulae of our previous and present liquid crystalline Pc-C$_{60}$ dyads (**1**, **2** and **3**) . * Our previous work (Ref. 29).

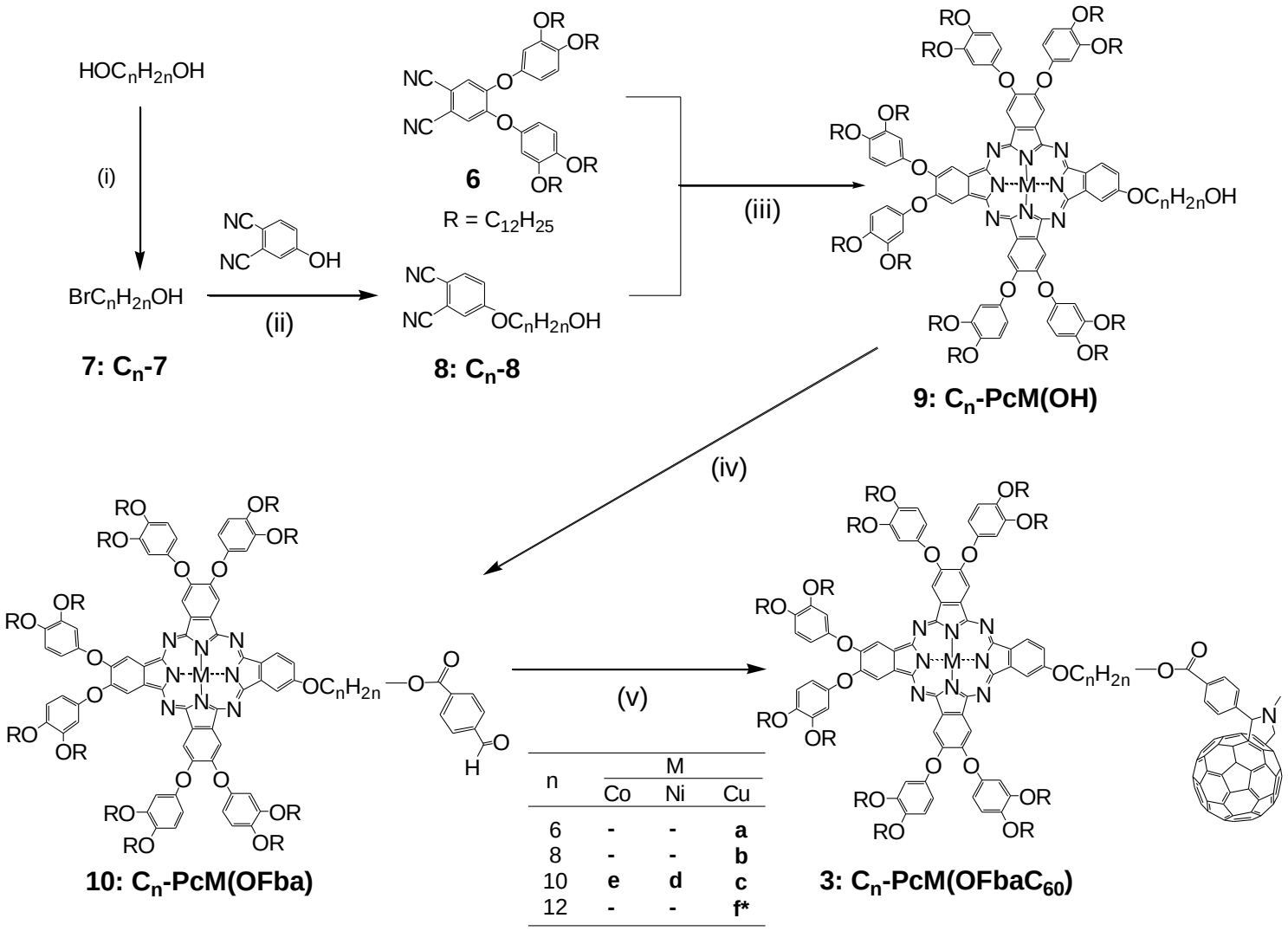


| n | M | | |
|---|---|---|---|
| | Co | Ni | Cu |
| 6 | - | - | **a** |
| 8 | - | - | **b** |
| 10 | **e** | **d** | **c** |
| 12 | - | - | **f*** |

**Scheme 1.** Synthetic route to **$C_n$-PcM(OH)** (**9a**~**f**), **$C_n$-PcM(OFba)** (**10a**~**f**) and **$C_n$-PcM(OFba$C_{60}$)** (**3a**~**f**). (i) 46%HBr $_{aq.}$/cyclohexane; (ii) $K_2CO_3$/DMF; (iii) $MCl_2$, DBU, 1-hexanol; (iv) *p*-formyl benzoic acid, DCC, DMAP, $CH_2Cl_2$; (v) N-methylglycine, $C_{60}$, toluene.* Our previous work (Ref. 29).

**Table 1.** Phase transition temperatures and enthalpy changes of **$C_n$-PcM(OH)** (**9a**~**f**), **$C_n$-PcCu(OFba)** (**10a**~**f**) and **$C_n$-PcCu(OFba$C_{60}$)** (**3a**~**f**).

| Compound | Phase T/ °C [ΔH/ kJ mol $^{-1}$] Phase [a)] Relaxation |
|---|---|
| **9a: $C_6$-PcCu(OH)** | 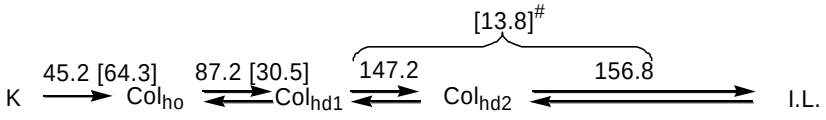  |
| **9b: $C_8$-PcCu(OH)** | 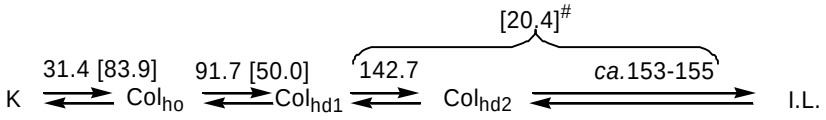  |
| **9c: $C_{10}$-PcCu(OH)** | 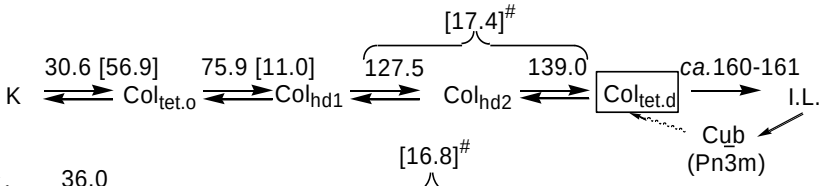  |
| **9d: $C_{10}$-PcNi(OH)** | 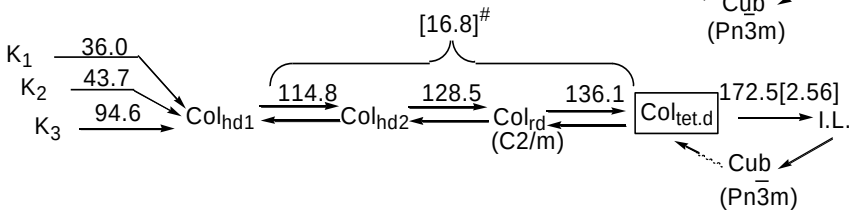  |
| **9e: $C_{10}$-PcCo(OH)** | 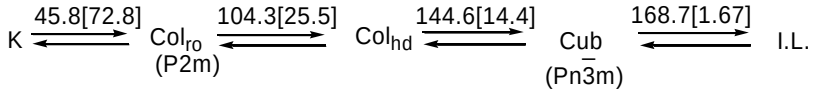  |
| **9f: $C_{12}$-PcCu(OH)*** | 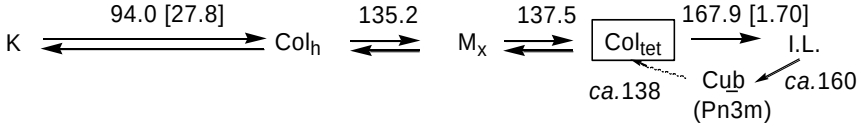  |
| **10a:$C_6$-PcCu(OFba)** | 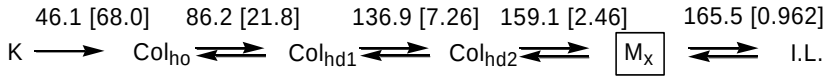  |
| **10b: $C_8$-PcCu(OFba)** | 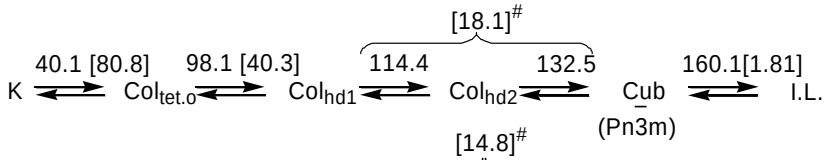  |
| **10c: $C_{10}$-PcCu(OFba)** | 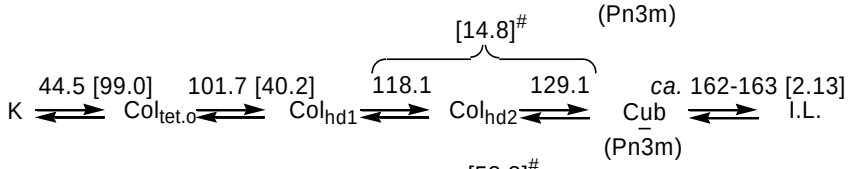  |
| **10d: $C_{10}$-PcNi(OFba)** | 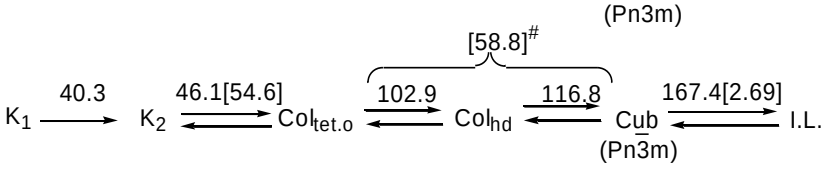  |
| **10e: $C_{10}$-PcCo(OFba)** | 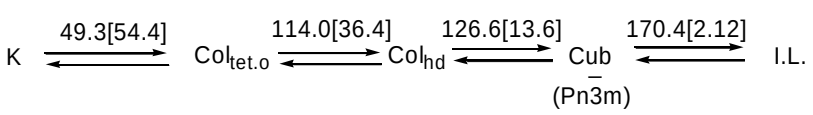  |
| **10f: $C_{12}$-PcCu(OFba)*** | 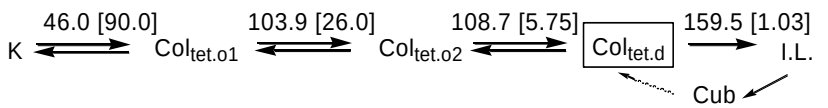  |

**Table 1 (continued)**

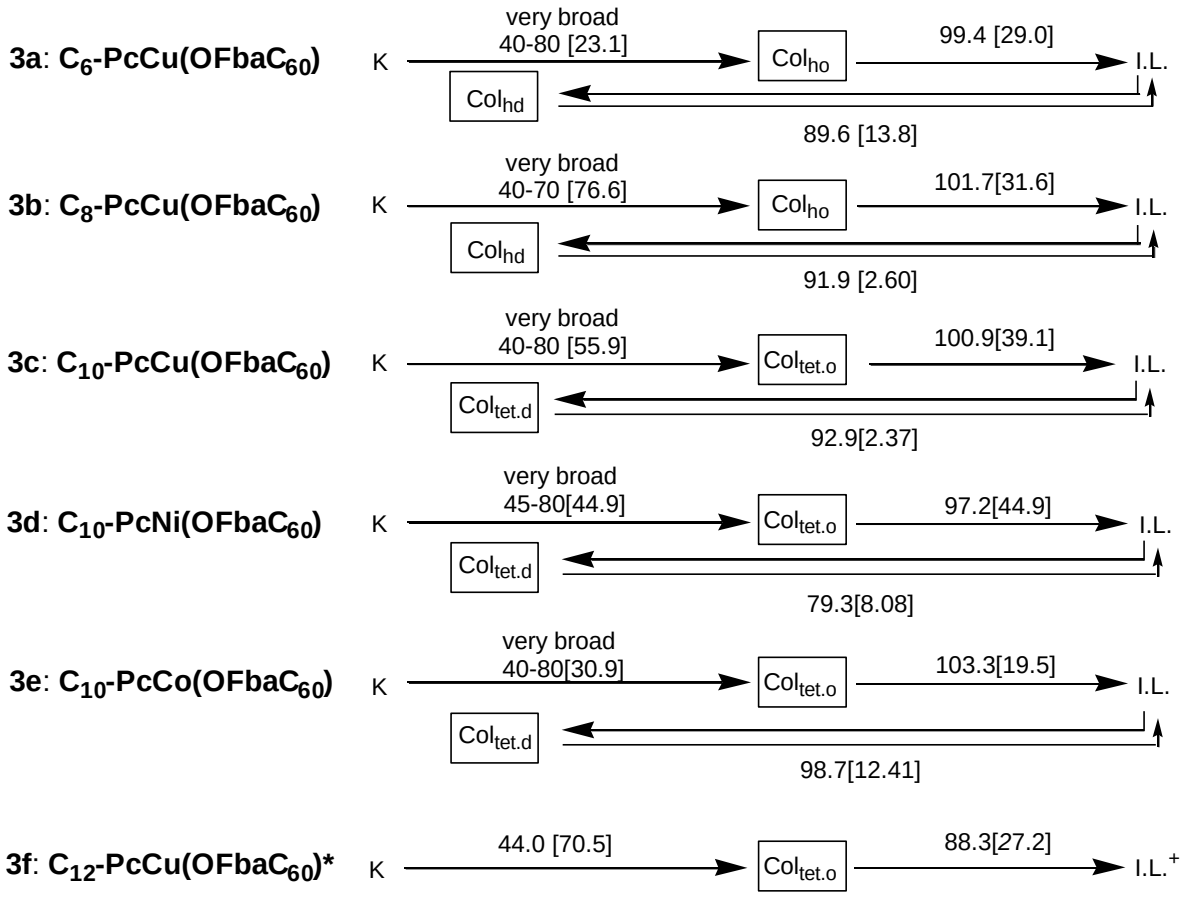


a) Phase nomenclature: K = crystal, $Col_{ho}$ = hexagonal ordered columnar mesophase, $Col_{hd}$ = hexagonal disordered columnar mesophase, $Col_{tet.o}$ = tetragonal ordered columnar mesophase, $Col_{tet.d}$ = tetragonal disordered columnar mesophase, $M_x$ = unidentified mesophase, Cub = cubic mesophase, I.L. = isotropic liquid, # = two peaks were too close to determine the enthalpy changes, ☐ = mesophase showing homeotropic alignment. + = gradual decomposition,
* = data from our previous work. See Ref. 29.

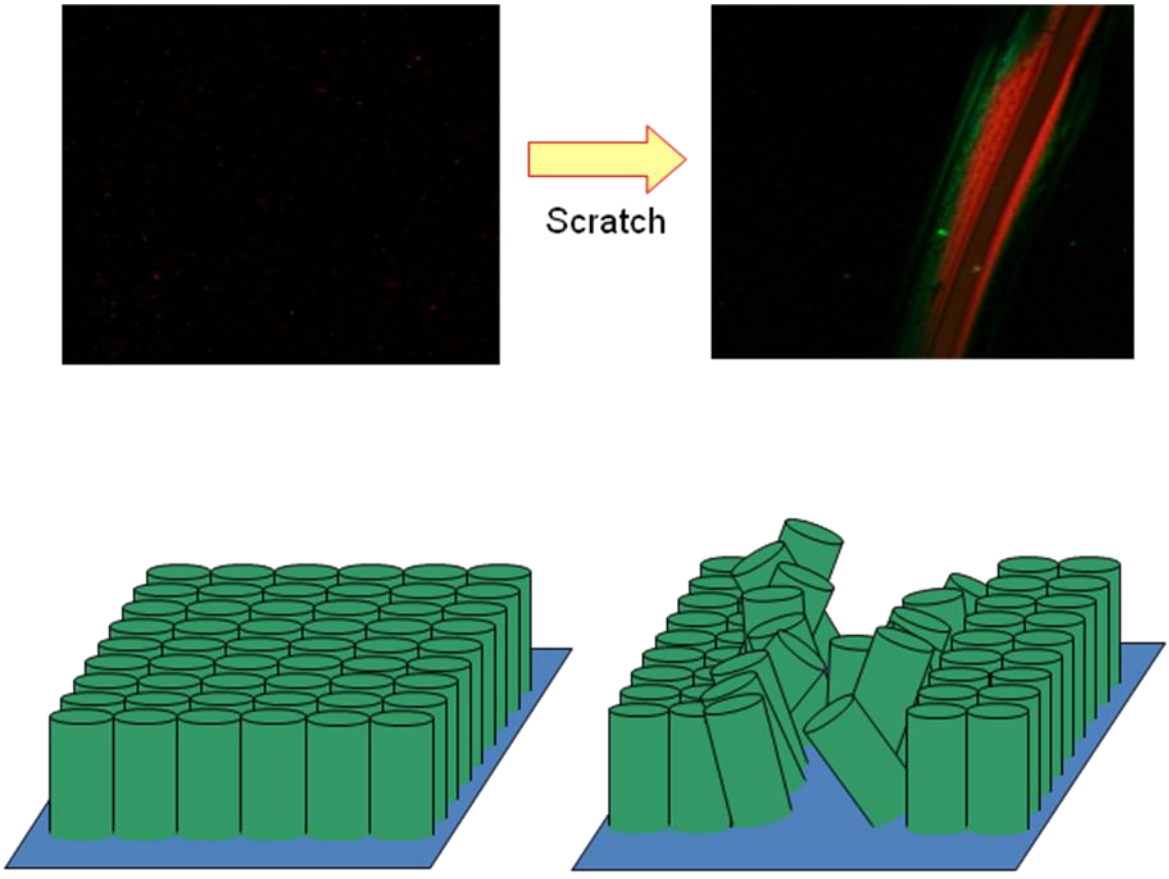


Fig. 2 Photomicrographs and columnar alignment models of the casted thin film of **$C_{10}$-PcCu(OFbaC$_{60}$)** (**3c**) showing perfect homeotropic alignment at 80 °C.

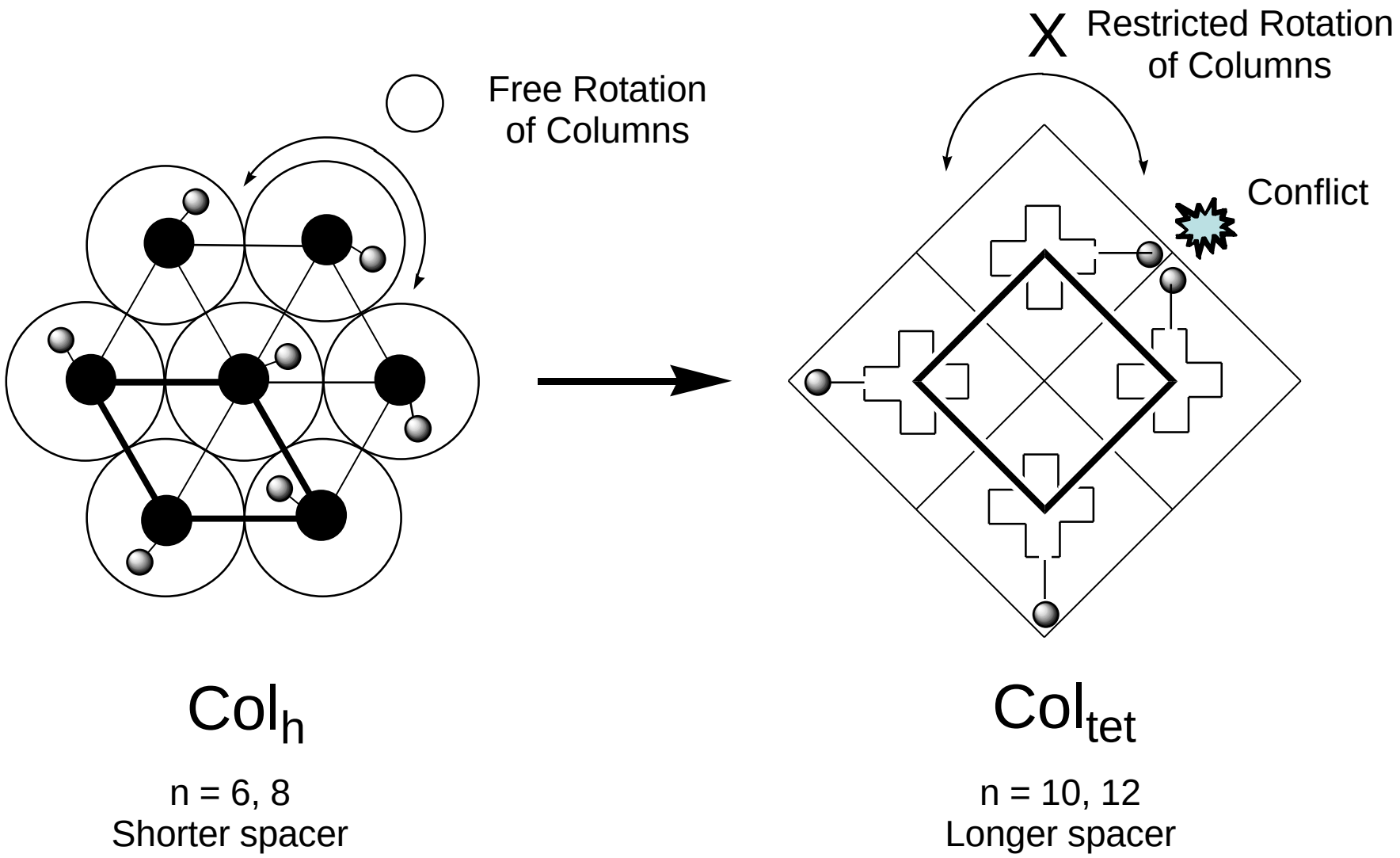


Fig. 3 Possible origin of formation of $Col_h$ and $Col_{tet}$ mesophases depending the spacer length between Pc and fullerene. O: rotation of columns is free; X: rotation of columns is restricted.

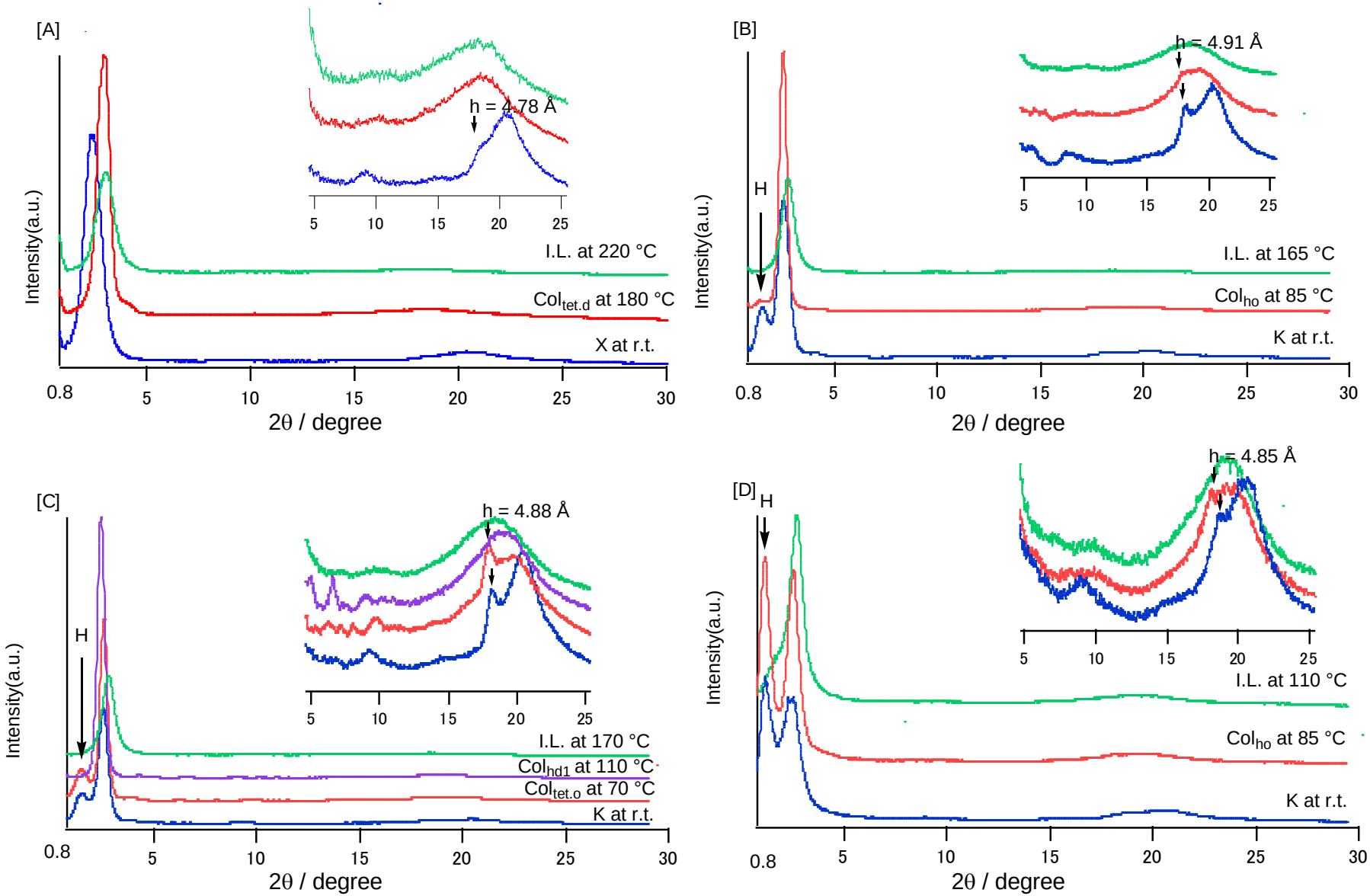


Fig. 4 Small angle X-ray diffraction patterns of [A] **(4 : 0)PcCu**, [B] **$C_8$-PcCu(OH)** (**9b**), [C] **$C_8$-PcCu(OFba)** (**10b**) and [D] **$C_8$-PcCu(OFba$C_{60}$)** (**3b**).

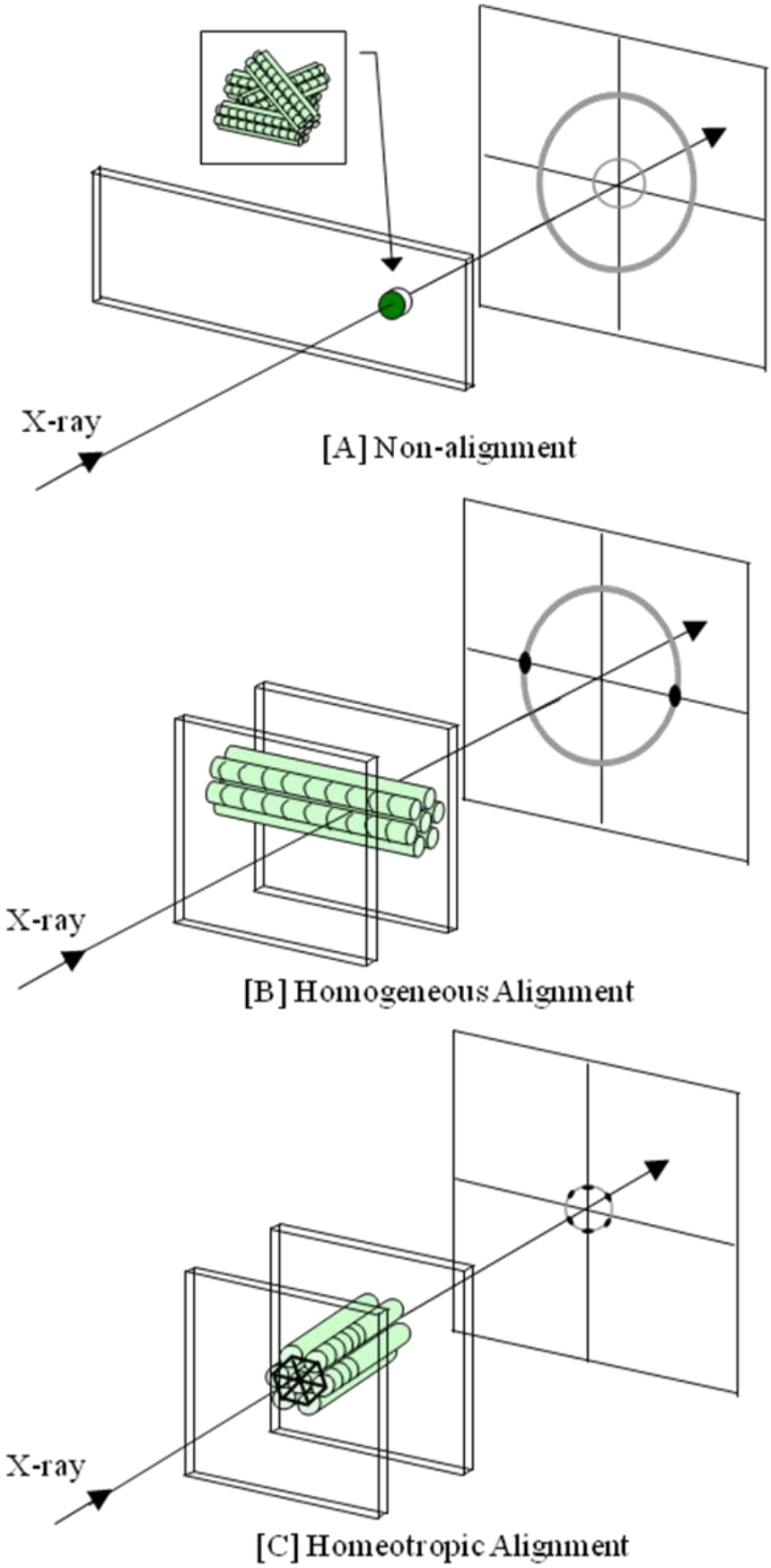


Fig. 5 Illustration of X-ray photographs of [A] non-alignment, [B] homogeneous alignment and [C] homeotropic alignment of ordered columns between two glass plates.

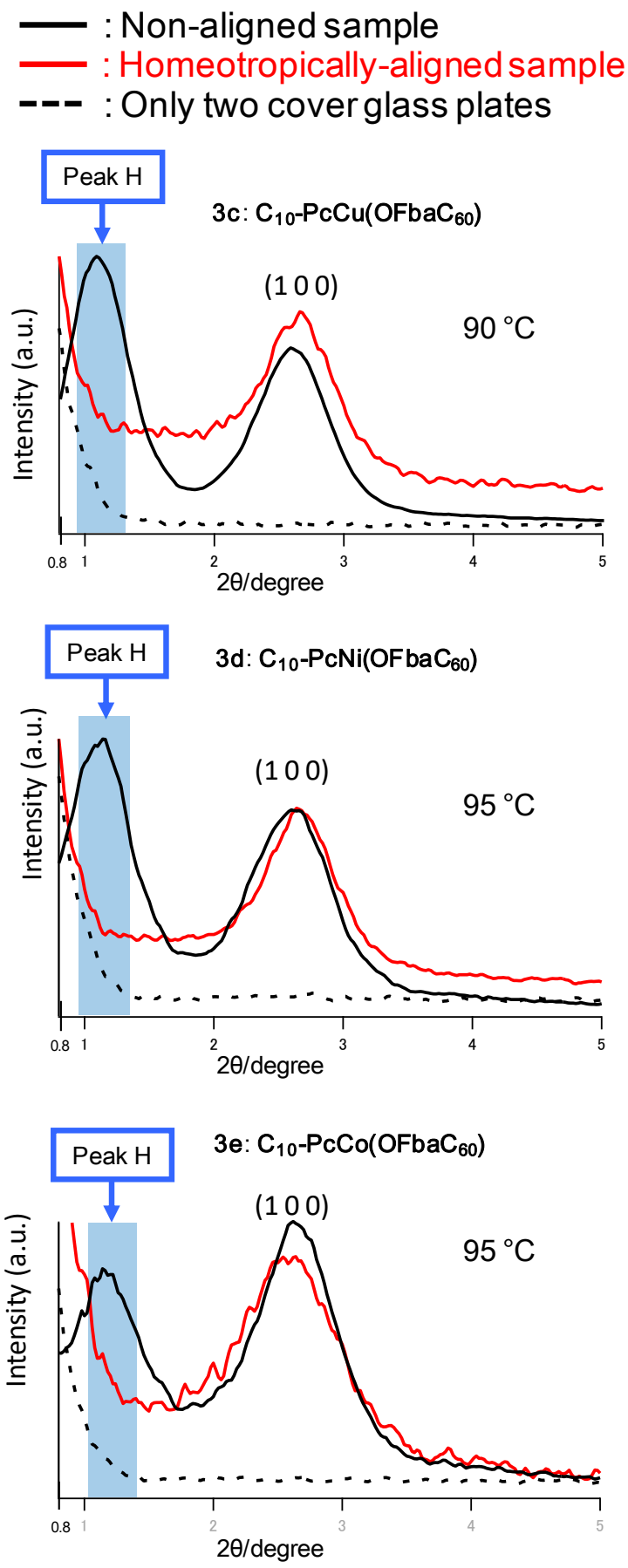


**Fig. 6** Small angle X-ray diffraction patterns of homeotropically aligned samples columns between two glass plates.

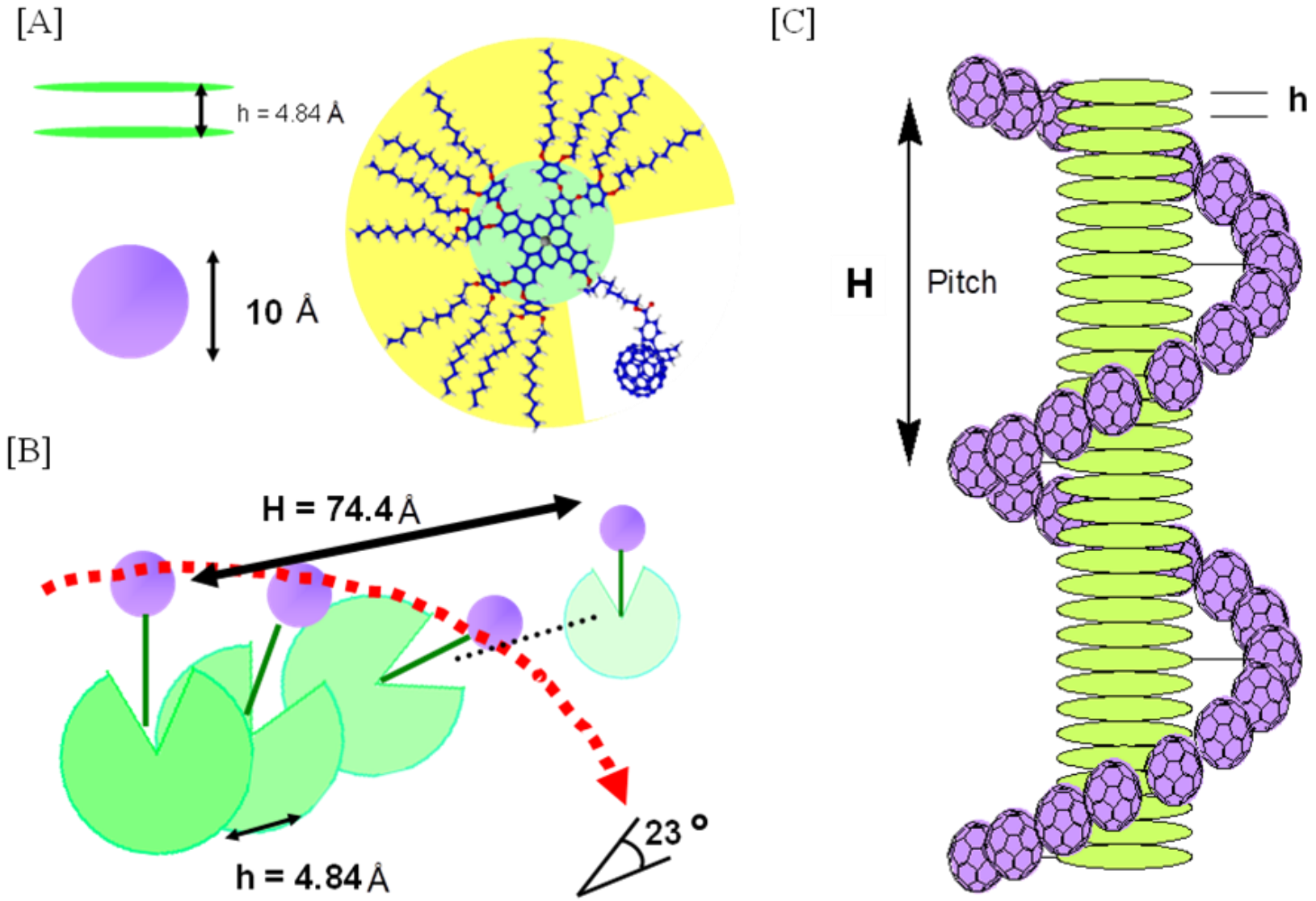


**Fig. 7** Proposed model of helical arrangement of fullerenes along with columns of phthalocyanine disks for for $C_{10}$-PcCu(OFbaC$_{60}$) (3c). At this present time, we could not determine whether the helicity of fullerenes is right-handed or left-handed.

**Table S1.** MALDI-TOF mass spectral data, elemental analysis data and yields of **$C_n$-PcM(OH)** (**9a~f**), **$C_n$-PcM(OFba)** (**10a~f**) and **$C_n$-PcM(OFba$C_{60}$)** (**3a~f**).

| Compound | Mol. formula (Mol. wt) | Mass observed | Elemental analysis: Found (Calcd.) (%) | | | Yield (%) |
|---|---|---|---|---|---|---|
| | | | C | H | N | |
| **9a: $C_6$-PcCu(OH)** | $C_{218}H_{340}N_8O_{20}Cu$ (3456.69) | 3457.00 | 76.05 (75.75) | 9.69 (9.91) | 3.40 (3.24 ) | 30.3 |
| **9b: $C_8$-PcCu(OH)** | $C_{220}H_{344}N_8O_{20}Cu$ (3484.74) | 3485.69 | 75.92 (75.83) | 10.01 (9.95) | 2.93 (3.22) | 29.7 |
| **9c: $C_{10}$-PcCu(OH)** | $C_{222}H_{348}N_8O_{20}Cu$ (3512.79) | 3514.66 | 75.85 (75.91) | 9.74 (9.99) | 3.30 (3.20) | 30.0 |
| **9d**: **$C_{10}$-PcNi(OH)** | $C_{220}H_{348}N_8O_{20}Ni$ (3508.18) | 3506.99 | 75.72 (76.01) | 9.82 (10.00) | 3.29 (3.19) | 17.3 |
| **9e**: **$C_{10}$-PcCo(OH)** | $C_{222}H_{348}N_8O_{20}Co$ (3508.40) | 3506.63 | 75.86 (76.01) | 10.25 (10.00) | 3.41 (3.19) | 15.4 |
| **9f: $C_{12}$-PcCu(OH)*** | $C_{224}H_{352}N_8O_{20}Cu$ (3540.85) | 3540.54 | 76.14 (75.98) | 10.21 (10.02) | 3.20 (3.16) | 29.5 |
| **10a:$C_6$-PcCu(OFba)** | $C_{226}H_{344}N_8O_{22}Cu$ (3588.80) | 3587.76 | 75.56 (75.64) | 9.41 (9.66) | 3.05 (3.12) | 95.1 |
| **10b: $C_8$-PcCu(OFba)** | $C_{228}H_{348}N_8O_{22}Cu$ (3616.86) | 3616.64 | 75.82 (75.72) | 9.72 (9.70) | 3.14 (3.10) | 63.1 |
| **10c: $C_{10}$-PcCu(OFba)** | $C_{230}H_{352}N_8O_{22}Cu$ (3644.91) | 3646.61 | 75.62 (75.79) | 9.85 (9.73) | 3.04 (3.07) | 57.0 |
| **10d**: **$C_{10}$-PcNi(OFba)** | $C_{230}H_{352}N_8O_{22}Ni$ (3640.30) | 3637.77 | 75.53 (75.89) | 9.51 (9.75) | 3.31 (3.08) | 90.3 |
| **10e**: **$C_{10}$-PcCo(OFba)** | $C_{230}H_{352}N_8O_{22}Co$ (3640.52) | 3637.98 | 76.20 (75.89) | 10.02 (9.75) | 2.82 (3.08) | 77.1 |
| **10f**: **$C_{12}$-PcCu(OFba)*** | $C_{232}H_{355}N_8O_{22}Cu$ (3671.96) | 3676.71 | 76.24 (75.89) | 10.14 (9.74) | 3.01 (3.05) | 65.0 |
| **3a**: **$C_6$-PcCu(OFbaC $_{60}$)** | $C_{288}H_{350}N_9O_{21}Cu$ (4337.54) | 4336.89<br>3616.64 | – | – | — | 93.7 |
| **3b**: **$C_8$-PcCu(OFbaC $_{60}$)** | $C_{290}H_{354}N_9O_{21}Cu$ (4365.59) | 4364.29<br>3645.83 | – | – | — | 76.7 |
| **3c**: **$C_{10}$-PcCu(OFbaC $_{60}$)** | $C_{292}H_{358}N_9O_{21}Cu$ (4393.65) | 4392.50<br>3673.53 | – | – | — | 86.2 |
| **3d**: **$C_{10}$-PcNi(OFbaC $_{60}$)** | $C_{292}H_{358}N_9O_{21}Ni$ (4389.04) | 4389.51<br>3668.70 | – | – | — | 89.5 |
| **3e**: **$C_{10}$-PcCo(OFbaC $_{60}$)** | $C_{292}H_{358}N_9O_{21}Co$ (4389.26) | 4386.12<br>3665.32 | – | – | — | 77.4 |
| **3f: $C_{12}$-PcCu(OFbaC $_{60}$)*** | $C_{294}H_{360}N_9O_{21}Cu$ (4419.69) | 4424.18<br>3705.23 | – | – | — | 85.1 |

* From our previous work (See Ref. 29).

**Table S2.** UV-vis spectral data in $CHCl_3$ of **$C_n$-PcM(OH)** (**9a~f**), **$C_n$-PcCu(OFba)** (**10a~f**) and **$C_n$-PcCu(OFba$C_{60}$)** (**3a~f**).

| Compound | Concentration† ( × $10^{-5}$ M.$l^{-1}$) | λ max, nm (logε) | | | | | |
|---|---|---|---|---|---|---|---|
| | | $C_{60}$ peak | Soret-band | | Q-band | | |
| | | | | | $Q_{0-1}$-band | * | $Q_{0-0}$-band |
| **9a: $C_6$-PcCu(OH)** | 0.98 | | 290.0 (4.9) | 341.6 (5.0) | 616.5 (4.7) | *ca.* 654 (sh) | 684.0 (5.4) |
| **9b: $C_8$-PcCu(OH)** | 1.0 | | 298.7 (4.8) | 340.2 (4.9) | 616.1 (4.6) | *ca.* 653 (sh) | 684.0 (5.3) |
| **9c: $C_{10}$-PcCu(OH)** | 1.0 | | 290.4 (4.9) | 339.5 (4.9) | 615.4 (4.7) | *ca.* 653 (sh) | 684.0 (5.4) |
| **9d**: **$C_{10}$-PcNi(OH)** | 0.26 | | 306.1 (4.9) | 330.1 (4.6) | 608.4 (4.5) | *ca.* 646 (sh) | 675.2 (5.2) |
| **9e**: **$C_{10}$-PcCo(OH)** | 0.23 | | 300.1 (5.0) | 323.4 (5.0) | 609.0 (4.6) | *ca.* 645 (sh) | 675.2 (5.3) |
| **9f: $C_{12}$-PcCu(OH)**$^{\$}$ | 1.8 | | 290.8 (4.9) | 340.2 (5.0) | 615.4 (4.7) | 651.8 (4.6) | 686.7 (5.3) |
| **10a: $C_6$-PcCu(OFba)** | 0.78 | | 289.3 (4.9) | 339.6 (4.9) | 615.1 (4.6) | *ca.* 651 (sh) | 684.7 (5.3) |
| **10b: $C_8$-PcCu(OFba)** | 1.0 | | 290.4 (4.9) | 339.5 (5.0) | 615.4 (4.7) | *ca.* 653 (sh) | 684.0 (5.4) |
| **10c: $C_{10}$-PcCu(OFba)** | 1.0 | | 290.4 (4.9) | 339.5 (5.0) | 616.1 (4.7) | *ca.* 653 (sh) | 684.0 (5.4) |
| **10d: $C_{10}$-PcNi(OFba)** | 0.22 | | 306.7 (5.1) | 328.8 (4.9) | 607.8 (4.7) | *ca.* 647 (sh) | 675.2 (5.4) |
| **10e: $C_{10}$-PcCo(OFba)** | 0.19 | | 301.4 (5.0) | 326.8 (5.0) | 609.7 (4.6) | *ca.* 647 (sh) | 675.2 (5.2) |
| **10f: $C_{12}$-PcCu(OFba)**$^{\$}$ | 1.6 | | 291.3 (4.9) | 341.3 (4.9) | 615.0 (4.6) | 652.5 (sh) | 685.0 (5.3) |
| **3a: $C_6$-PcCu(OFba$C_{60}$)** | 0.23 | 252.8 (5.4) | 282.9 (5.2) | 338.2 (5.1) | 619.0 (4.7) | *ca.* 658 (sh) | 688.3 (5.3) |
| **3b: $C_8$-PcCu(OFba$C_{60}$)** | 0.27 | 256.4 (5.3) | 290.6 (5.2) | 341.8 (5.1) | 618.7 (4.7) | *ca.* 653 (sh) | 686.3 (5.3) |
| **3c: $C_{10}$-PcCu(OFba$C_{60}$)** | 0.20 | 255.6 (5.2) | 289.8 (5.1) | 339.0 (5.0) | 616.6 (4.6) | *ca.* 656 (sh) | 685.6 (5.3) |
| **3d: $C_{10}$-PcNi(OFba$C_{60}$)** | 0.16 | 254.0 (5.2) | 306.7 (5.1) | 330.1 (4.9) | 610.4 (4.5) | *ca.* 647 (sh) | 676.5 (5.2) |
| **3e: $C_{10}$-PcCo(OFba$C_{60}$)** | 0.11 | 246.0 (5.3) | 288.0 (5.2) | 323.4 (5.1) | 611.1 (4.5) | *ca.* 647 (sh) | 679.8 (5.2) |
| **3f: $C_{12}$-PcCu(OFba$C_{60}$)**$^{\$}$ | 0.52 | 255.6 (5.2) | 292.7 (sh) | 340.3 (sh) | 618.1 (4.7) | 652.2 (sh) | 684.9 (5.2) |

†: In chloroform. *: Aggregation band of Q0–0 band. sh: Shoulder. $: Data from our previous work (see Ref. 29)

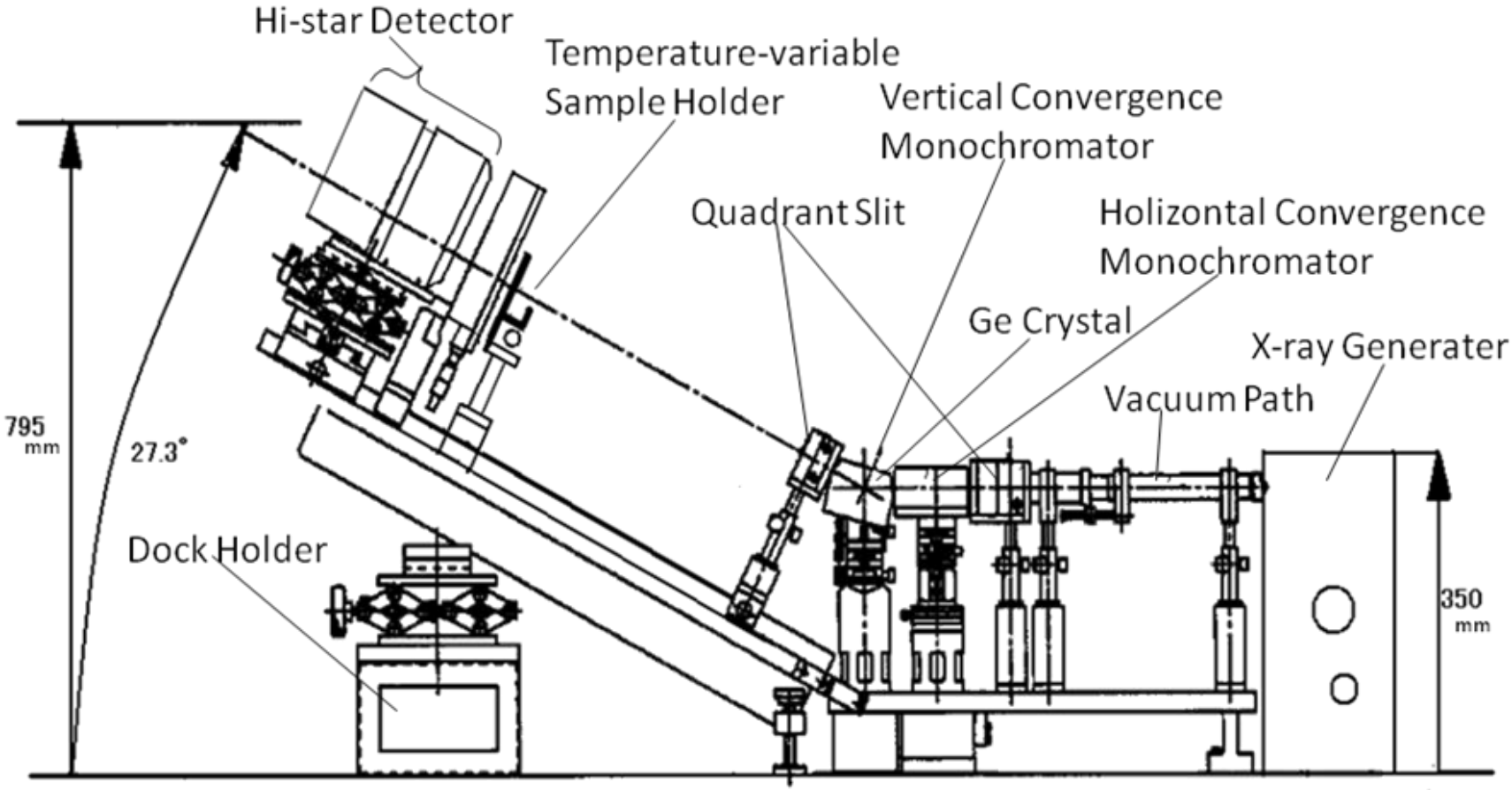


**Fig. S1. Setup of Small-Angle X-ray Scattering (Bruker MAC SAXS ) equipped with a temperature-variable sample holder.**

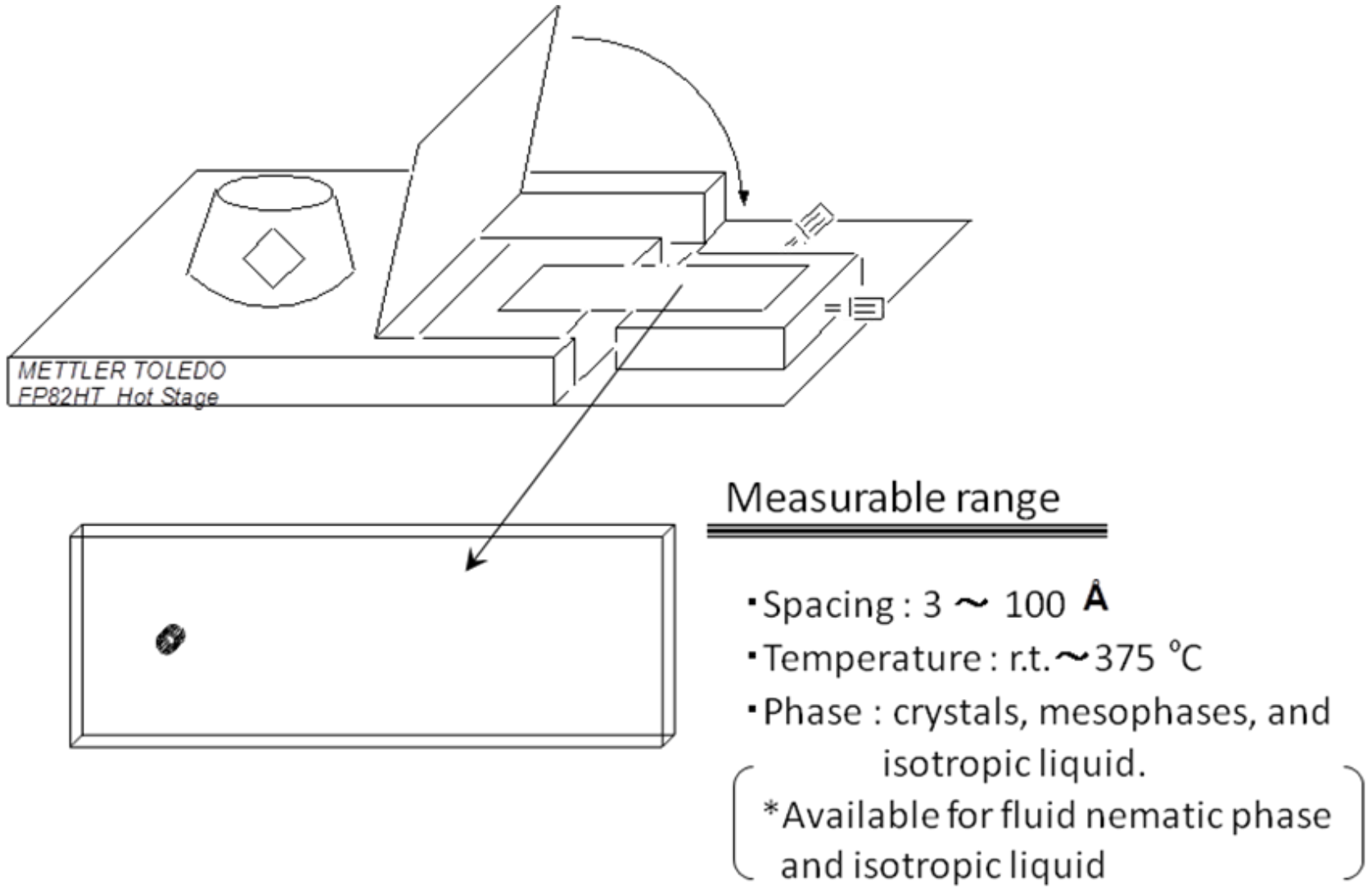


**Fig. S2. Setup of the temperature-variable sample holder.**

**Table S3.** X-ray data of the **$C_n$-PcM(OH)** derivatives (**9a~f**).

| Compound Mesophase | Lattice constants, Å | Spacing, Å | | Miller indices (*h k l*) |
|---|---|---|---|---|
| | | Observed | Calculated | |
| **9a: $C_6$-PcCu(OH)** | | | | |
| $Col_{ho}$ at 66 °C | a = 39.5 | 54.7 | - | H |
| | h = 4.84 | 34.2 | 34.2 | (1 0 0) |
| | Z = 1.1 for $\rho$ = 1.0 | 20.8 | 19.8 | (1 1 0) |
| | | *ca.*9.6 | - | ph |
| | | 4.84 | - | h |
| | | *ca.*4.3 | - | # |
| $Col_{hd1}$ at 112 °C | a = 40.4 | 35.0 | 35.0 | (1 0 0) |
| | | 20.9 | 20.2 | (1 1 0) |
| | | 18.1 | 17.5 | (2 0 0) |
| | | 13.5 | 13.2 | (2 1 0) |
| | | *ca.*9.9 | - | ph |
| | | *ca.*4.6 | - | # |
| $Col_{hd2}$ at 148 °C | a = 39.8 | 34.5 | 34.5 | (1 0 0) |
| | | 20.4 | 19.9 | (1 1 0) |
| | | 17.3 | 17.2 | (2 0 0) |
| | | 13.1 | 13.0 | (2 1 0) |
| | | 11.6 | 11.5 | (3 0 0) |
| | | *ca.*9.5 | - | ph |
| | | *ca.*4.6 | - | # |
| **9b: $C_8$-PcCu(OH)** | | | | |
| $Col_{ho}$ at 85 °C | a = 40.6 | 58.9 | - | H |
| | h = 4.91 | 35.2 | 35.2 | (1 0 0) |
| | Z = 1.2 for $\rho$ = 1.0 | 20.3 | 20.3 | (1 1 0) |
| | | 17.4 | 17.6 | (2 0 0) |
| | | 13.3 | 13.3 | (2 1 0) |
| | | *ca.*9.9 | - | ph |
| | | 4.91 | - | h |
| | | *ca.*4.4 | - | # |
| $Col_{hd1}$ at 120 °C | a = 40.8 | 35.3 | 35.3 | (1 0 0) |
| | | 20.9 | 20.4 | (1 1 0) |
| | | 13.5 | 13.3 | (2 1 0) |
| | | *ca.*4.7 | - | # |
| $Col_{hd2}$ at 150 °C | a = 39.2 | 34.0 | 34.0 | (1 0 0) |
| | | 19.8 | 19.6 | (1 1 0) |
| | | 17.0 | 17.0 | (2 0 0) |
| | | 12.9 | 12.8 | (2 1 0) |
| | | *ca.*4.6 | - | # |

# = Halo of the molten alkoxy chains. h = Stacking distance. H = Helical pitch. ph = Halo of the molten phenyl groups.

**Table S3**. (Continued).

| Compound Mesophase | Lattice constants, Å | Spacing, Å | | Miller indices (*h k l*) |
|---|---|---|---|---|
| | | Observed | Calculated | |
| **9c: $C_{10}$-PcCu(OH)** | | | | |
| $Col_{tet.o}$ at 80 °C | a = 33.4 | 57.8 | - | H |
| | h = 4.85 | 33.4 | 33.4 | (1 0 0) |
| | Z = 0.93 for $\rho$ = 1.0 | 23.2 | 23.6 | (1 1 0) |
| | | 4.85 | - | h |
| | | *ca*.4.5 | - | # |
| $Col_{hd1}$ at 120 °C | a = 38.9 | 33.7 | 33.7 | (1 0 0) |
| | | 19.5 | 19.9 | (1 1 0) |
| | | 16.8 | 17.2 | (2 0 0) |
| | | 12.7 | 13.1 | (2 1 0) |
| | | *ca*.9.6 | - | ph |
| | | *ca*.4.6 | - | # |
| $Col_{hd2}$ at 145 °C | a = 38.3 | 33.2 | 33.2 | (1 0 0) |
| | | 19.8 | 19.2 | (1 1 0) |
| | | 12.8 | 12.5 | (2 1 0) |
| | | *ca*.9.4 | - | ph |
| | | *ca*.4.7 | - | # |
| - | | | | |
| Cub (Pn3m) at 152 °C | a = 70.8 | 35.3 | 35.4 | (2 0 0) |
| | Z ≈ 61 for $\rho$ = 1.0 | 32.0 | 31.6 | (2 1 0) |
| | | 16.5 | 16.7 | (3 3 0) |
| | | *ca*.4.6 | - | # |
| **9d: $C_{10}$-PcNi(OH)** | | | | |
| $Col_{hd1}$ at 105 °C | a = 40.6 | 35.1 | 35.1 | (1 0 0) |
| | | 20.7 | 20.3 | (1 1 0) |
| | | 17.8 | 17.6 | (2 0 0) |
| | | 13.5 | 13.3 | (2 1 0) |
| | | 9.83 | 9.74 | (3 1 0) |
| | | *ca*.4.6 | - | # |
| $Col_{hd2}$ at 122 °C | a = 40.1 | 34.8 | 34.8 | (1 0 0) |
| | | 20.8 | 20.1 | (1 1 0) |
| | | 17.2 | 17.4 | (2 0 0) |
| | | 13.2 | 13.1 | (2 1 0) |
| | | 9.60 | 9.64 | (3 1 0) |
| | | *ca*.4.6 | - | # |
| $Col_{rd}$(C2/m) at 132 °C | a = 65.0 | 32.5 | 32.5 | (2 0 0) |
| | b = 46.3 | 23.2 | 23.2 | (0 2 0) |
| | | 19.3 | 18.9 | (2 2 0) |
| | | 16.3 | 16.3 | (4 0 0) |
| | | 12.5 | 12.5 | (5 1 0) |

| | | | | |
|---|---|---|---|---|
| | | *ca.*4.7 | - | # |
| $Col_{tet.d}$ at 154 °C | a = 31.3 | 31.3 | 31.3 | (1 0 0) |
| | | 22.1 | 22.1 | (1 1 0) |
| | | *ca.*4.6 | - | # |
| - | | | | |
| Cub (Pn3m) at 154 °C | a = 103.0 | 36.4 | 36.0 | (2 2 0) |
| | Z ≈ 262 for $\rho$ = 1.0 | 33.4 | 33.9 | (2 2 1) |
| | | 32.2 | 32.2 | (3 1 0) |
| | | 31.0 | 30.7 | (3 1 1) |
| | | 22.5 | 22.7 | (4 2 0) |
| | | 21.9 | 21.7 | (3 3 2) |
| | | *ca.* 4.6 | - | # |

**Table S3**. (Continued).

| Compound Mesophase | Lattice constants, Å | Spacing, Å | | Miller indices (*h k l*) |
|---|---|---|---|---|
| | | Observed | Calculated | |
| **9e: $C_{10}$-PcCo(OH)** | | | | |
| $Col_{ro}$(P2m) at 75 °C | a = 33.6 | 64.3 | - | H |
| | b = 31.3 | 33.6 | 33.6 | (1 0 0) |
| | h = 4.83 | 31.3 | 31.3 | (0 1 0) |
| | Z = 0.88 for $\rho$ = 1.0 | 21.4 | 22.9 | (1 1 0) |
| | | 17.1 | 16.8 | (2 0 0) |
| | | 15.5 | 15.7 | (0 2 0) |
| | | 4.83 | - | h |
| | | *ca.*4.5 | - | # |
| $Col_{hd}$ at 125 °C | a = 39.3 | 34.0 | 34.0 | (1 0 0) |
| | | 19.7 | 19.6 | (1 1 0) |
| | | 17.0 | 17.0 | (2 0 0) |
| | | 13.1 | 12.8 | (2 1 0) |
| | | 9.58 | 9.42 | (3 1 0) |
| | | *ca.*4.7 | - | # |
| - | | | | |
| Cub (Pn3m) at 157 °C | a = 105.6 | 35.2 | 35.2 | (2 1 1) |
| | Z ≈ 202 for $\rho$ = 1.0 | 33.6 | 33.4 | (2 2 0) |
| | | 32.3 | 31.8 | (3 1 0) |
| | | 19.9 | 20.0 | (3 1 1) |
| | | 19.0 | 19.0 | (2 2 2) |
| | | *ca.*4.8 | - | # |
| **9f: $C_{12}$-PcCu(OH)*** | | | | |
| $Col_{hd}$ at 120 °C | a = 40.7 | 34.5 | 34.5 | (1 0 0) |
| | | 20.3 | 19.9 | (1 1 0) |
| | | 17.3 | 17.2 | (2 0 0) |
| | | 13.1 | 13.0 | (2 1 0) |
| | | 11.6 | 11.5 | (3 0 0) |

| | | | | |
|---|---|---|---|---|
| | | *ca.*4.4 | - | # |
| $Col_{tet.d}$ at 160 $^{o}$C | a = 30.9 | 30.7 | 30.9 | (1 0 0) |
| | | 21.9 | 21.9 | (1 1 0) |
| | | *ca.*9.6 | - | # |
| | | *ca.*4.7 | - | # |
| - | | | | |
| Cub (Pn3m) at 154 $^{o}$C on cooloing | a = 144 | 38.4 | 38.4 | (3 2 1) |
| | | 34.0 | 34.0 | (3 3 0) |
| | | 33.2 | 33.2 | (3 3 1) |
| | | 32.0 | 32.0 | (4 2 0) |
| | | 30.9 | 30.9 | (3 3 2) |
| | | 22.6 | 22.7 | (6 2 1) |
| | | *ca.* 8.6 | - | # |
| | | *ca.* 4.6 | - | # |
| | | *ca.* 3.5 | - | h |

**Table S4.** X-ray data of the $C_n$-**PcM(OFba)** derivatives (**10a~f**).

| Compound Mesophase | Lattice constants, Å | Spacing, Å | | Miller indices (*h k l*) |
|---|---|---|---|---|
| | | Observed | Calculated | |
| **10a: (12, 6)PcCu(OFba)** | | | | |
| $Col_{ho}$ at 66 °C | a = 41.7 | 59.1 | - | H |
| | h = 4.82 | 36.1 | 36.1 | (1 0 0) |
| | Z ≈ 1.2 for $\rho$ = 1.0 | 20.7 | 20.8 | (1 1 0) |
| | | 13.6 | 13.6 | (2 1 0) |
| | | *ca.*8.8 | - | ph |
| | | 4.82 | - | h |
| | | *ca.*4.5 | - | # |
| $Col_{hd1}$ at 111 °C | a = 41.7 | 36.1 | 36.1 | (1 0 0) |
| | | 20.5 | 20.8 | (1 1 0) |
| | | 13.6 | 13.6 | (2 1 0) |
| | | *ca.*9.8 | - | ph |
| | | *ca.*4.6 | - | # |
| $Col_{hd2}$ at 148 °C | a = 39.7 | 34.4 | 34.4 | (1 0 0) |
| | | 16.8 | 17.2 | (2 0 0) |
| | | 12.9 | 13.0 | (2 1 0) |
| | | *ca.*9.3 | - | ph |
| | | *ca.*4.7 | - | # |
| $M_X$ at 162 °C | | 32.2 | - | - |
| | | 21.3 | - | - |
| | | *ca.* 9.0 | - | ph |
| | | *ca.* 4.7 | - | # |
| **10b: $C_8$-PcCu(OFba)** | | | | |
| $Col_{tet.o}$ at 70 °C | a = 32.9 | 55.2 | - | H |
| | h = 4.88 | 33.7 | 32.9 | (1 0 0) |
| | Z = 0.92 for $\rho$ =1.0 | 23.2 | 23.2 | (1 1 0) |
| | | *ca.*10.9 | - | ph |
| | | 4.88 | - | h |
| | | *ca.*4.4 | - | # |
| $Col_{hd1}$ at 110 °C | a = 41.6 | 35.0 | 36.1 | (1 0 0) |
| | | 20.8 | 20.8 | (1 1 0) |
| | | 13.5 | 13.6 | (2 1 0) |
| | | *ca.*4.6 | - | # |
| $Col_{hd2}$ at 120 °C | a = 40.4 | 35.0 | 35.0 | (1 0 0) |
| | | 20.3 | 20.2 | (1 1 0) |
| | | 17.9 | 17.5 | (2 0 0) |
| | | 13.1 | 13.2 | (2 1 0) |
| | | *ca.*4.5 | - | # |

| | | | | |
|---|---|---|---|---|
| Cub (Pn3m) at 145 °C | a = 109.1 | 38.7 | 38.6 | (1 1 1) |
| | Z ≈ 216 for $\rho$ = 1.0 | 36.2 | 36.4 | (2 2 1) |
| | | 32.9 | 32.9 | (3 1 1) |
| | | 31.8 | 31.5 | (2 2 2) |
| | | *ca.*4.5 | - | # |

# = Halo of the molten alkoxy chains. h = Stacking distance. H = Helical pitch. ph = Halo of the molten phenyl groups.

**Table S4**. (Continued).

| Compound Mesophase | Lattice constants, Å | Spacing, Å | | Miller indices (*h k l*) |
|---|---|---|---|---|
| | | Observed | Calculated | |
| **10c: $C_{10}$-PcCu(OFba)** | | | | |
| $Col_{tet.o}$ at 75 °C | a = 33.7 | 58.9 | - | H |
| | h = 4.87 | 33.7 | 33.7 | (1 0 0) |
| | Z = 0.91 for $\rho$ = 1.0 | 24.1 | 23.8 | (1 1 0) |
| | | *ca.*9.3 | - | ph |
| | | 4.87 | - | h |
| | | *ca.*4.4 | - | # |
| $Col_{hd1}$ at 105 °C | a = 40.8 | 35.3 | 35.3 | (1 0 0) |
| | | 20.6 | 20.4 | (1 1 0) |
| | | 17.7 | 17.7 | (2 0 0) |
| | | 13.3 | 13.3 | (2 1 0) |
| | | *ca.*9.5 | - | ph |
| | | *ca.*4.6 | - | # |
| $Col_{hd2}$ at 127 °C | a = 39.5 | 34.2 | 34.2 | (1 0 0) |
| | | 20.0 | 19.8 | (1 1 0) |
| | | 12.9 | 12.9 | (2 2 0) |
| | | *ca.*4.7 | - | # |
| - | | | | |
| Cub (Pn3m) at 140 °C | a = 105.1 | 37.1 | 37.2 | (2 2 0) |
| | Z ≈ 192 for $\rho$ = 1.0 | 35.3 | 35.0 | (2 2 1) |
| | | 31.5 | 31.7 | (3 1 1) |
| | | *ca.*4.6 | - | # |
| **10d: $C_{10}$-PcNi(OFba)** | | | | |
| $Col_{tet.o}$ at 75 °C | a = 33.6 | 61.7 | - | H |
| | h = 4.89 | 33.6 | 33.6 | (1 0 0) |
| | Z = 0.91 for r = 1.0 | 23.1 | 23.8 | (1 1 0) |
| | | 14.8 | 15 | (2 1 0) |
| | | 10.6 | 10.6 | (3 1 0) |
| | | 4.89 | - | h |
| | | ca.4.5 | - | # |
| $Col_{hd}$ at 110 °C | a = 38.8 | 33.6 | 33.6 | (1 0 0) |

| | | | | |
|---|---|---|---|---|
| | | 19.7 | 19.4 | (1 1 0) |
| | | 16.8 | 16.8 | (2 0 0) |
| | | 13.0 | 12.7 | (2 1 0) |
| | | 9.41 | 9.32 | (3 1 0) |
| | | ca.4.7 | - | # |
| - | a = 136.5 | 39.4 | 39.6 | (2 2 2) |
| Cub (Pn3m) at 160 °C | Z ≈ 421 for $\rho$ = 1.0 | 37.0 | 36.6 | (3 2 1) |
| | | 34.0 | 34.3 | (4 0 0) |
| | | 31.5 | 31.5 | (3 3 1) |
| | | 30.6 | 30.7 | (4 2 0) |

**Table S4**. (Continued).

| Compound Mesophase | Lattice constants, Å | Spacing, Å | | Miller indices (*h k l*) |
|---|---|---|---|---|
| | | Observed | Calculated | |
| **10e: $C_{10}$-PcCo(OFba)** | | | | |
| $Col_{tet.o}$ at 75 °C | a = 32.8 | 59.1 | - | H |
| | h = 4.85 | 32.8 | 32.8 | (1 0 0) |
| | Z = 0.87 for $\rho$ = 1.0 | 22.2 | 23.2 | (1 1 0) |
| | | 14.4 | 14.7 | (2 1 0) |
| | | 10.9 | 10.9 | (3 0 0) |
| | | 9.43 | 9.11 | (3 2 0) |
| | | 4.85 | - | h |
| | | *ca.*4.6 | - | # |
| $Col_{hd1}$ at 120 °C | a = 39.7 | 34.4 | 34.4 | (1 0 0) |
| | | 20.0 | 19.8 | (1 1 0) |
| | | 17.5 | 17.2 | (2 0 0) |
| | | 13.3 | 13.0 | (2 1 0) |
| | | 11.6 | 11.5 | (3 0 0) |
| | | 9.67 | 9.54 | (3 1 0) |
| | | *ca.*4.7 | - | # |
| - | | | | |
| Cub (Pn3m) at 160 °C | a = 109.5 | 38.7 | 39.0 | (2 2 0) |
| | Z ≈ 217 for $\rho$ = 1.0 | 36.7 | 36.7 | (3 0 0) |
| | | 34.3 | 34.8 | (3 1 0) |
| | | 33.2 | 33.2 | (3 1 1) |
| | | 29.9 | 29.4 | (3 2 1) |
| | | *ca.*4.5 | - | # |
| **10f: $C_{12}$-PcCu(OFba)*** | | | | |
| $Col_{tet.o1}$ at 80 °C | a = 32.3 | 61.6 | - | H |
| | h = 4.85 | 32.7 | 32.3 | (1 0 0) |
| | Z = 0.85 for $\rho$ = 1.0 | 22.9 | 22.9 | (1 1 0) |
| | | *ca.*12 | - | (2 2 0) + (3 0 0) |

| | | | | |
|---|---|---|---|---|
| | | 4.85 | - | h |
| | | *ca.*4.3 | - | # |
| $Col_{tet.o2}$ at 107 $^{o}$C | a = 35.0 | 58.0 | - | H |
| | | 35.0 | 35.0 | (1 0 0) |
| | | 23.2 | 24.8 | (1 1 0) |
| | | 17.7 | 17.5 | (2 0 0) |
| | | *ca.*12 | *ca.*12 | (2 2 0) + (3 0 0) |
| | | 8.73 | 8.76 | (4 0 0) |
| | | *ca.*4.4 | - | # |
| $Col_{tet.d}$ at 145 $^{o}$C | a = 31.1 | 31.1 | 31.1 | (1 0 0) |
| | | 22.5 | 22.0 | (1 1 0) |
| | | *ca.*12 | - | (2 2 0) + (3 0 0) |
| | | *ca.*4.7 | - | # |
| - | | | | |
| Cub (Pn3m) at 155 $^{o}$C | a = 128 | 38.7 | 38.7 | (3 1 1) |
| | | 37.1 | 37.0 | (2 2 2) |
| | | 34.0 | 33.9 | (3 2 1) |
| | | 30.7 | 30.6 | (3 3 0) |
| | | *ca.*12.2 | - | # |
| | | *ca.*4.4 | - | # |

**Table S5.** X-ray data of the **Cn-PcM(OFbaC$_{60}$)** derivatives (**3a~f**).

| Compound Mesophase | Lattice constants, Å | Spacing, Å | | Miller indices (*h k l*) |
|---|---|---|---|---|
| | | Observed | Calculated | |
| **3a: C$_6$-PcCu(OFbaC$_{60}$)** | | | | |
| Col$_{ho}$ at 85 $^{o}$C | a = 41.4 | 77.9 | - | H |
| | h = 4.85 | 35.9 | 35.9 | (1 0 0) |
| for the virgin sample | Z = 1.0 for $\rho$ = 1.0 | 21.6 | 20.7 | (1 1 0) |
| | | *ca.*10.0 | - | ph |
| | | 4.85 | - | h |
| | | *ca.*4.5 | - | # |
| Col$_{hd}$ at 85 $^{o}$C | a = 39.2 | 53.8 | - | H |
| | | 34.0 | 34.0 | (1 0 0) |
| for the non-virgin sample | | 20.6 | 19.6 | (1 1 0) |
| | | *ca.*9.5 | - | ph |
| | | *ca.*4.6 | - | # |
| **3b: C$_8$-PcCu(OFbaC$_{60}$)** | | | | |
| Col$_{ho}$ at 85 $^{o}$C | a = 40.8 | 75.8 | - | H |
| | h = 4.85 | 35.3 | 35.3 | (1 0 0) |
| for the virgin sample | Z = 0.96 for $\rho$ = 1.0 | 21.7 | 20.4 | (1 1 0) |
| | | *ca.*9.7 | - | ph |
| | | 4.85 | - | h |
| | | *ca.*4.5 | - | # |
| Col$_{hd}$ at 60 $^{o}$C | a = 39.5 | 65.7 | - | H |
| | | 34.2 | 34.2 | (1 0 0) |
| for the non-virgin sample | | 19.9 | 19.8 | (1 1 0) |
| | | *ca.*9.4 | - | ph |
| | | *ca.*4.5 | - | # |
| **3c: C$_{10}$-PcCu(OFbaC$_{60}$)** | | | | |
| Col$_{tet\cdot o}$ at 90 $^{o}$C | a = 33.4 | 74.4 | - | H |
| | h = 4.84 | 33.4 | 33.4 | (1 0 0) |
| for the virgin sample | Z = 0.74 for $\rho$ =1.0 | 23.6 | 23.6 | (1 1 0) |
| | | 14.4 | 14.9 | (2 1 0) |
| | | *ca* 9.5 | | ph |
| | | 4.84 | - | h |
| | | *ca.*4.5 | - | # |
| Col$_{tet.d}$ at 90 $^{o}$C | a = 32.4 | 55.4(sh) | - | H |
| | | 32.4 | 32.4 | (1 0 0) |
| for the non-virgin sample | | 22.9 | 22.9 | (1 1 0) |
| | | ca. 9.2 | - | ph |
| | | ca. 4.6 | - | # |

# = Halo of the molten alkoxy chains. h = Stacking distance between the monomers. H = helical pitch of the fullerenes. ph = Halo of the molten phenyl groups.

**Table S5.** (continured)

| Compound Mesophase | Lattice constants, Å | Spacing, Å | | Miller indices (*h k l*) |
|---|---|---|---|---|
| | | Observed | Calculated | |
| **3d: $C_{10}$-PcNi(OFbaC$_{60}$)** | | | | |
| $Col_{tet.o}$ at 95 °C | a = 32.6 | 77.8 | - | H |
| | h = 4.85 | 32.6 | 32.6 | (1 0 0) |
| for the virgin sample | Z = 0.99 for $\rho$ = 1.4 | 22.4 | 23.0 | (1 1 0) |
| | | 4.85 | - | h |
| | | *ca*.4.5 | - | # |
| $Col_{tet.d}$ at rt | a = 31.3 | 58.2 | - | H |
| | | 31.3 | 31.3 | (1 0 0) |
| | | 21.5 | 22.1 | (1 1 0) |
| | | *ca*.4.4 | - | # |
| **3e: $C_{10}$-PcCo(OFbaC$_{60}$)** | | | | |
| $Col_{tet.o}$ at 95 °C | a = 32.5 | 75.8 | - | H |
| | h = 4.84 | 32.5 | 32.5 | (1 0 0) |
| for the virgin sample | Z = 1.0 for $\rho$ = 1.4 | 22.3 | 22.9 | (1 1 0) |
| | | 4.84 | - | h |
| | | *ca*.4.5 | - | # |
| $Col_{tet.d}$ at rt | a = 32.5 | 61.6 | - | H |
| | | 32.5 | 32.5 | (1 0 0) |
| | | 22.3 | 23.0 | (1 1 0) |
| | | *ca*.4.5 | - | # |
| **3f: $C_{12}$-PcCu(OFbaC$_{60}$)** | | | | |
| $Col_{tet.o}$ at 90 °C | a = 33.2 | 75.4 | - | H |
| | h = 4.85 | 33.2 | 33.2 | (1 0 0) |
| | Z = 0.73 for $\rho$ = 1.0 | 23.4 | 23.5 | (1 1 0) |
| | | 11.5 | 11.7 | (2 2 0) |
| | | 4.85 | - | h |
| | | *ca*.4.5 | - | # |
| $Col_{tet.d}$ at 60 °C | a = 33.2 | 65.7 | - | H |
| | | 33.2 | 33.2 | (1 0 0) |
| for the non-virgin sample | | 23.5 | 23.5 | (1 1 0) |
| | | 11.8 | 11.7 | (2 2 0) |
| | | *ca*.4.4 | - | # |

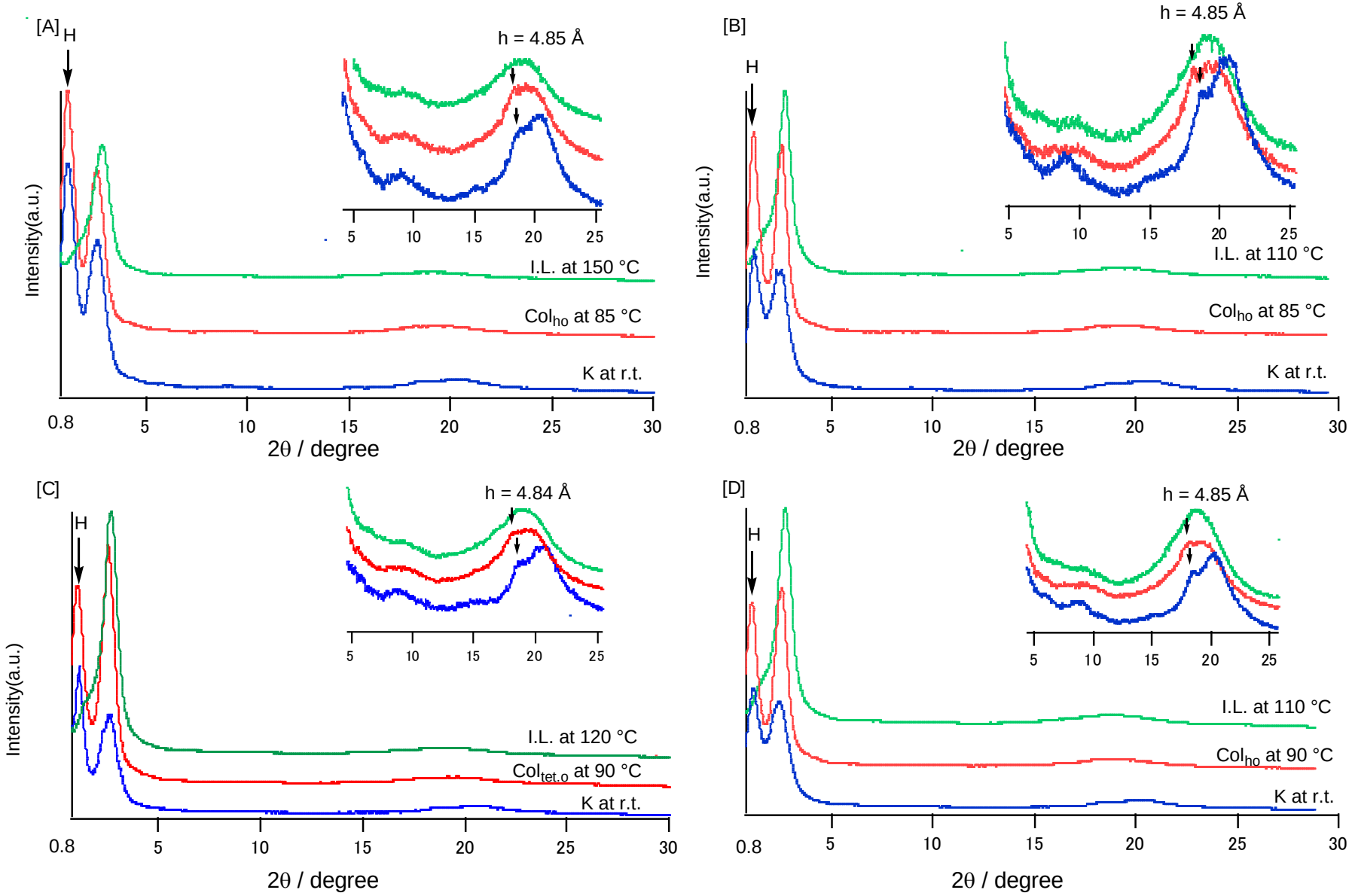


Fig. S3 Small angle X-ray diffraction patterns of [A] **$C_6$-PcCu(OFbaC$_{60}$)** (**3a**); [B] **$C_8$-PcCu(OFbaC$_{60}$)** (**3b**); [C] **$C_{10}$-PcCu(OFbaC$_{60}$)** (**3c**); [D] **$C_{12}$-PcCu(OFbaC$_{60}$)** (**3f**).